Physics Lib.

OCT 15 1948

REGISTERED No. M. 3121

PROCEEDINGS

OF THE

INDIAN ACADEMY

OF SCIENCES

VOL. XXVIII] *SECTION A* [NO. 2

AUGUST, 1948

Price Rs. 2 or 3 Sh. *Annual Subscription Rs. 18*

PRINTED AT THE BANGALORE PRESS, BANGALORE CITY, BY G. SRINIVASA RAO, SUPERINTENDENT, AND PUBLISHED BY THE INDIAN ACADEMY OF SCIENCES, BANGALORE

NUCLEAR OXIDATION IN THE FLAVONES AND RELATED COMPOUNDS

Part XIV. Constitution of Quercetagitrin

By S. Rajagopalan and T. R. Seshadri, F.A.Sc.

(From the Department of Chemistry, Andhra University, Waltair)

Received July 1, 1948

Two important species of the Marigold, *Tagetes erecta*[1] and *Tagetes patula*[2] have been examined in the past with regard to their flower pigments. The difference in species is clearly indicated in the nature of the colouring matter present. The first contains mainly the monoglucoside, quercetagitrin along with some quantity of its aglucone, quercetagetin. On the other hand the flowers of *Tagetes patula* yield only patuletin which is a mono-methyl ether of quercetagetin. Thus the close botanical relationship between the two species and at the same time their species difference is paralleled on the chemical side. The pigments of both flowers are based on quercetagetin, one containing the monoglucoside and the other the monomethyl ether.

The constitution of patuletin was first surmised[3] as the 6-methyl-ether (I) from its properties and reactions and it was later confirmed[4] definitely by the unequivocal synthesis of its penta-ethyl ether (II).

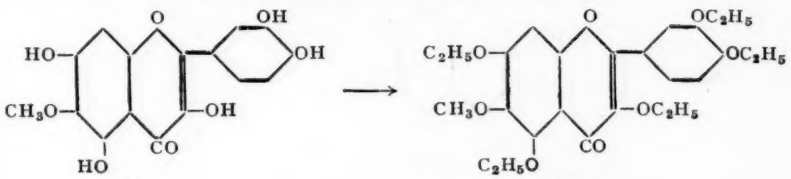

(I) (II)

With regard to quercetagitrin, its constitution as the 7-monoglucoside was originally arrived at only by the elimination of other possibilties.[1] After the complete methylation of the glucoside through the acetate and subsequent hydrolysis, a pentamethyl quercetagetin was obtained which gave, on decomposition with alkali, veratric acid thus eliminating the possibility of existence of the free hydroxyl group in the side phenyl nucleus. Comparison with the already known 5-hydroxy compound showed that it was different and eliminated this position also from consideration. The lack of prominent ferric chloride colour showed that there was no free

hydroxyl even in the 3-position. Out of the two still left, the position 7 (formula IV) was considered to have the free hydroxyl group because the allyl ether of the compound underwent Claisen migration smoothly. This would not have been possible if the 6-position was concerned. But no confirmation by synthesis was provided for the constitution of this pentamethyl quercetagetin and eventually for the glucoside, quercetagitrin. This has now been supplied by experiments described in this paper.

Quercetagitrin has now been more conveniently methylated using excess of dimethyl sulphate and potassium carbonate in acetone medium. The pentamethyl quercetagetin obtained by the hydrolysis of the methylated glucoside has been further ethylated and this mixed ether (A) has been shown to be identical with a synthetic sample of 7-ethoxy-3 : 5 : 6 : 3′ : 4′-pentamethoxy flavone (V). The starting point for this synthesis is 2-hydroxy-4-ethoxy-ω : 6-dimethoxy acetophenone (VI) and the stages are given by the following formulæ. Thus it is confirmed that the pentamethyl quercetagetin has formula (IV) and quercetagitrin formula (III).

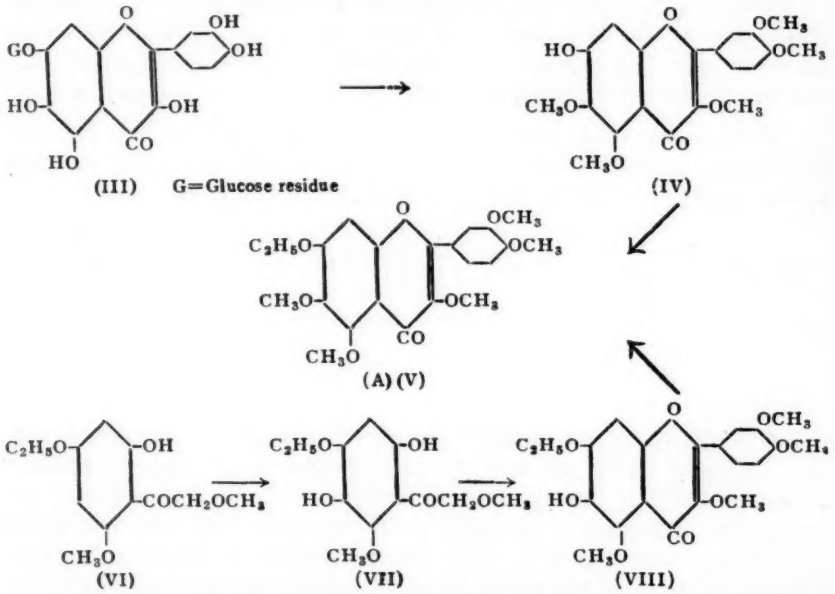

The above mentioned starting material (VI) has been most conveniently obtained from quercimeritrin, the well-known monoglucoside of quercetin. Its constitution as a 7-glucoside (IX) was originally advanced by Attree and Perkin[5] (see also Rao and Seshadri[6]) by a process of elimination. They

showed that the derived tetramethyl quercetin did not have the free hydroxyl group in the side phenyl nucleus by a study of its decomposition products and that it was not in the 3 or the 5-position by comparison with the required synthetic compounds. No confirmation of the constitution (X) by synthesis has been made so far. This has now been done by the ethylation of the tetramethyl quercetin and by the synthesis of the resulting mixed ether (XI) by a straightforward method. 3 : 3′ : 4′-*O*-trimethyl quercetin (XII)[7] which is readily obtained by the Allan-Robinson condensation of ω-methoxy-phloracetophenone with the anhydride and sodium salt of veratric acid, is partially ethylated using just one mol. of ethyl iodide and the product (XIII) is a monoethyl ether whose reactions indicate that the resistant 5-hydroxyl group is still free. Final methylation with excess of dimethyl sulphate yields the required mixed ether of quercetin (XI). The various stages are indicated by the following formulæ:

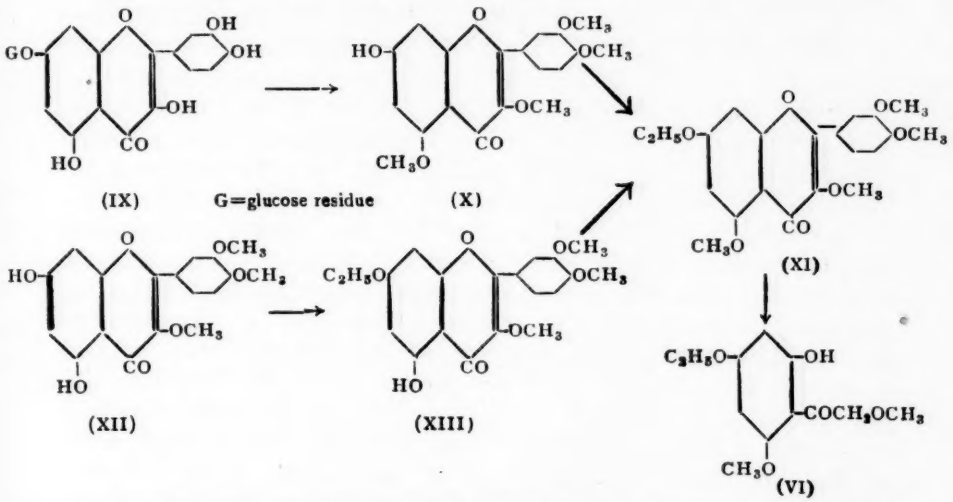

Fission using alcoholic alkali of the above mixed ether (XI) obtained either from quercimeritrin or by the synthetic method yielded besides veratric acid the required 2-hydroxy-4-ethoxy-ω : 6-dimethoxy acetophenone (VI) and this was employed as the starting material for the synthesis of the above mentioned pentamethyl-monoethyl quercetagetin. As a purely synthetic method of obtaining this ketone, the synthesis of *O*-7-ethyl-3 : 5-dimethyl galangin (XVI) and its fission with alcoholic alkali has also been carried out. This is far more convenient than preparing the quercetin derivative synthetically.

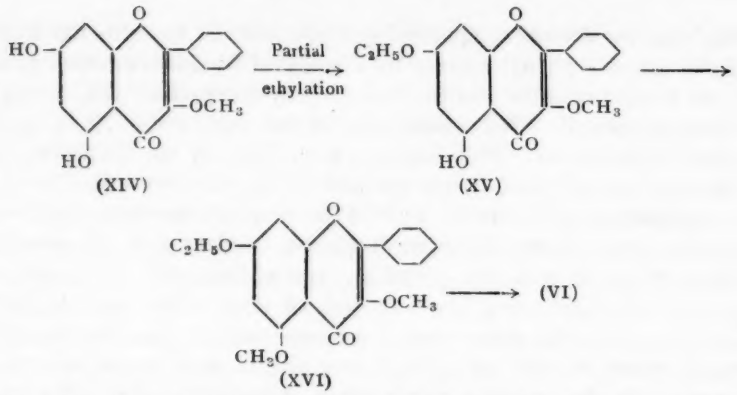

The above experiments emphasise the relationship between quercimeritrin and quercetagitrin, both being 7-glucosides. Further from the results it will be clear that the species difference between *T. erecta* and *T. patula* is not only exhibited in the way a hydroxyl group is protected but this is also exhibited in the particular position involved, 7- in the glucoside and 6- in the methyl ether. This choice of the position for the glucoside formation and methylation in the case of 5:6:7-hydroxy-flavones and flavonols is rather interesting. As somewhat parallel cases may be mentioned the derivatives of scutellarein and baicalein. In their partial methyl ethers the 6-position is used in preference to 7. For example, the 6-methyl ether of baicalein (oroxylin-A) is found in *Oroxylum indicum* and the 6:4′-dimethyl ether of scutellare in occurs in *Linaria vulgaris*. Regarding the glucuronides, baicalin and scutellarin Armstrong and Armstrong in their well-known monograph on glycosides[8] state that the glucuronic acid is in both cases thought to be attached in position 6. No evidence is however mentioned in support of this opinion. On the other hand the experiments of Shibata and Hattori[9] would show that the constitution of baicalin should be as the 7-glucuronide of baicalin.

Experimental

Quercetin-tetramethyl-ether (X) *from Quercimeritrin.*

Quercimeritrin required for this work was obtained from the flower petals of the Cambodia cotton plant (*Gossypium hirsutum*).[10] It (1·0 g.) was suspended in dry acetone (150 c.c.) and anhydrous potassium carbonate (5 g.) and dimethyl sulphate (3 c.c.) were added and the mixture was heated under reflux for a period of 30 hours. The potassium salts were filtered and washed with warm acetone. From the filtrate the solvent was distilled

off and water added to the residue. The methyl ether separated as a semi-solid mass; it gave no colour with alcoholic ferric chloride. It was directly boiled with 7% aqueous sulphuric acid for two hours. It first went into solution and a colourless solid soon separated out. The product was filtered and washed with water. On crystallisation from alcohol the tetramethyl ether was obtained as narrow rectangular plates, melting at 284–85°; Attree and Perkin[5] and Rao and Seshadri[6] recorded the same melting point. It dissolved in aqueous sodium hydroxide to give an yellow colour but did not give any colour with alcoholic ferric chloride. Yield, 0·4 g. (Found: C, 63·7; H, 5·4; $C_{19}H_{18}O_7$ requires C, 63·7; H, 5·0%.) Its acetate melted at 174–75°.

Monoethyl-tetramethyl-quercetin (*XI*)

The above tetramethyl quercetin (0·2 g.) was dissolved in dry acetone (50 c.c.), freshly ignited potassium carbonate (5 g.) and ethyl iodide (0·5 c.c.) added and the mixture refluxed for 15 hours. The potassium salts were filtered and washed with warm acetone. On removing the solvent from the filtrate and adding water, the ethyl ether separated as a colourless solid. It crystallised from ethyl acetate as broad rhombohedral plates and prisms melting at 159–60°. It was insoluble in aqueous sodium hydroxide and did not give any colour with alcoholic ferric chloride. The mixed melting point with a synthetic sample of 7-ethoxy-3:5:3′:4′-tetramethoxy-flavone was undepressed. (Found: C, 65·6; H, 5·8; $C_{21}H_{22}O_7$ requires C, 65·3; H, 5·7%).

7-*Ethoxy*-5-*hydroxy*-3:3′:4′-*trimethoxy-flavone* (*XIII*)

5:7-Dihydroxy-3:3′:4′-trimethoxy-flavone[7] (0·5 g.) in dry acetone (50 c.c.) was treated with anhydrous potassium carbonate (5·0 g.) and ethyl-iodide (1·1 mol.; 0·3 c.c.) and refluxed for 8 hours. After filtration, the solution was concentrated whereby the crude partially ethylated compound was obtained as a pale yellow solid. It crystallised from absolute alcohol as narrow rectangular plates (pale yellow) melting at 134–35°. It gave a reddish-brown colour with alcoholic ferric chloride, was sparingly soluble in aqueous sodium hydroxide and dissolved in concentrated sulphuric acid to give a bright yellow solution. Yield, 0·4 g. (Found: C, 64·7; H, 5·0; $C_{20}H_{20}O_7$ requires C, 64·5; H, 5·4%).

7-*Ethoxy*-3:5:3′:4′-*tetramethoxy-flavone* (*XI*)

The above 5-hydroxy compound (0·2 g.) was further methylated in dry acetone (50 c.c.) solution using anhydrous potassium carbonate (5 g.) and freshly distilled dimethyl sulphate (0·5 c.c.) and heating under reflux for

20 hours. The product was readily obtained as a colourless solid. It crystallised from ethyl acetate as broad rectangular plates melting at 158–60°. Yield, 0·2 g. (Found: C, 65·1; H, 5·3; $C_{21}H_{22}O_7$ requires C, 65·3; H, 5·7%). It was identical with the monoethyl-tetramethyl quercetin obtained from quercimeritrin.

Pentamethyl quercetagetin from quercetagitrin (IV)

The glucoside required for this purpose was isolated from the flowers of *Tagetes erecta* using a modification of the method adopted by Rao and Seshadri.[1] The alcoholic extract of the petals was concentrated removing as much alcohol as possible. The residue was treated with excess of water, heated and resinous matter filtered off. The clear solution was concentrated to a small bulk and repeatedly extracted with ether in order to remove quercetagetin. When the aqueous solution was allowed to stand saturated with ether, the glucoside separated in the course of a few weeks. It was filtered and washed with ether and recrystallised from pyridine.

It (0·5 g.) was methylated as in the case of quercimeritrin using dry acetone (100 c.c.), anhydrous potassium carbonate (7 g.) and freshly distilled dimethyl sulphate (3 c.c.) and refluxing the mixture for 30 hours. When the filtrate was concentrated to remove the solvent and water added no solid separated. Hence the solution was rendered 7% acid by the addition of the requisite amount of sulphuric acid and gently boiled for 2 hours, when the aglucone separated out slowly. It was filtered and washed with water. On crystallisation from alcohol the monohydroxy compound was obtained as colourless long plates and needles, melting at 234–35° (Rao and Seshadri[1]). Yield, 0·2 g.

Monoethyl-pentamethyl-quercetagetin (A)

The above pentamethyl ether (0·15 g.) was ethylated using dry acetone (50 c.c.), anhydrous potassium carbonate (3 g.) and ethyl iodide (0·3 c.c.) and refluxing the mixture for 20 hours. The potassium salts were filtered off and washed with warm acetone. When the filtrate was concentrated to remove the solvent and water added, a brown sticky solid separated out. It was left in the ice-chest overnight when the product came out as an amorphous powder. Crystallisation from aqueous alcohol yielded colourless plates melting at 127–28°. The melting point was not depressed by admixture with a synthetic sample of 7-ethoxy-pentamethoxy flavone (V). Yield, 0·15g. It was insoluble in aqueous sodium hydroxide and did not give any colour with alcoholic ferric chloride. (Found; C, 63·2; H, 5·6; $C_{22}H_{24}O_8$ requires C, 63·5; H, 5·8%).

2-*Hydroxy*-4-*ethoxy*-ω: 6-*dimethoxy-acetophenone* (*VI*)

7-Ethoxy-3: 5: 3′: 4′-tetramethoxy-flavone obtained from quercimeritrin or synthetically (1·0 g.) was treated with absolute alcoholic potash (40 c.c., 8%) and the solution refluxed for 6 hours. As much of the alcohol as possible was removed under reduced pressure and the remaining solution diluted with water. It was then rendered acidic with dilute sulphuric acid and ether extracted. The ether extract was shaken with aqueous sodium bicarbonate in order to remove veratric acid and then evaporated when the ketone separated as a colourless solid. Crystallisation from alcohol yielded it as thin rectangular plates and needles melting at 105–6°. It gave a reddish brown colour with alcoholic ferric chloride and dissolved in aqueous sodium hydroxide to give an yellow solution. Yield 0·5 g. (Found: C, 60·0; H, 6·5; $C_{12}H_{16}O_5$ requires C, 60·0; H, 6·7%.)

2: 5-*Dihydroxy*-4-*ethoxy*-ω: 6-*dimethoxy-acetophenone* (*VII*)

To a stirred solution of the above ketone (1·0 g.) in aqueous sodium hydroxide (1·0 g. in 15 c.c.) was added dropwise a solution of potassium persulphate (1·2 g. in 30 c.c. of water) in the course of two hours, the temperature being kept at 15–20°. After 24 hours the brown aqueous solution was neutralised with dilute hydrochloric acid to congo red and ether extracted to remove the unreacted ketone. To the aqueous solution was then added concentrated hydrochloric acid (20 c.c.) and sodium sulphite (2 g.) and the mixture heated in a boiling water-bath for half an hour. It was then cooled and extracted with ether. On distilling off the ether a viscous liquid was obtained which did not solidify even after leaving in the refrigerator for a number of days. Hence it was employed directly for the subsequent condensation. Yield, 0·25 g.

It gave a greenish brown colour with alcoholic ferric chloride and an yellow solution with aqueous sodium hydroxide.

7-*Ethoxy*-3: 5: 6: 3′: 4′-*pentamethoxy flavone* (*V*)

An intimate mixture of the ketone (VII) (1·0 g.), veratric anhydride (6·0 g.) and sodium veratrate (2·5 g.) was heated under reduced pressure at 170–80° for 4 hours. The dark brown product was dissolved in hot alcohol (25 c.c.) and refluxed with an aqueous solution of potassium hydroxide (3 g. in 3 c.c. of water) for 30 minutes. The solvent was removed under reduced pressure and the residue dissolved in water. After saturation with carbon dioxide the solution was extracted with ether. On evaporating the ether solution the flavone was obtained as a viscous oil. It gave an olive green colour with ferric chloride indicating partial demethylation in the

5-position and an alcoholic solution of the substance gave a deep red colour with magnesium and hydrochloric acid. It was directly employed for the subsequent methylation by dissolving in dry acetone (30 c.c.) and boiling with anhydrous potassium carbonate (6 g.) and dimethyl sulphate (2·5 c.c.) for 20 hours. After filtration, the filtrate was concentrated and treated with water. The semi-solid mass thus obtained was taken up in ether and the ether solution evaporated. The residue was crystallised from benzene-petroleum ether when the 7-ethoxy-pentamethoxy flavone was obtained as rectangular plates melting at 127–28°. Yield, 0·5 g. It was insoluble in aqueous sodium hydroxide and did not give any colour with alcoholic ferric chloride. (Found: C, 63·6; H, 5·8; $C_{22}H_{24}O_8$ requires C, 63·5; H, 5·8%.)

7-Ethoxy-5-hydroxy-3-methoxy-flavone (*XV*)

Galangin-3-methyl ether[11] (2·0 g.) in dry acetone (100 c.c.) was treated with anhydrous potassium carbonate (2 g.) and ethyl iodide (1 mol., 1 c.c.) and the contents were refluxed for 6 hours. The potassium salts were filtered and washed with warm acetone. On concentrating the filtrate a semi-solid mass was obtained which when treated with a little alcohol yielded a yellow solid. It crystallised from alcohol as narrow rectangular plates (yellow) melting at 125–6°. It gave a reddish-brown colour with alcoholic ferric chloride. Yield, 1·5 g. (Found: C, 69·3; H, 5·1; $C_{18}H_{16}O_5$ requires C, 69·2; H, 5·1%.)

7-Ethoxy-3: 5-dimethoxy flavone (*XVI*)

The above 5-hydroxy compound (0·5 g.) was methylated in dry acetone (50 c.c.) with excess of dimethyl sulphate (0·5 c.c.) and anhydrous potassium carbonate (5 g.) by boiling the mixture for 10 hours. The methyl ether crystallised from alcohol as fine needles melting at 128–29°. It did not give any colour with alcoholic ferric chloride and was insoluble in aqueous sodium hydroxide. Yield, 0·4 g. (Found: C, 69·5; H, 5·2; $C_{19}H_{18}O_5$ requires C, 69·9; H, 5·5%).

This flavone (1·0 g.) was subjected to fission using absolute alcoholic potash (40 c.c., 8%) and the product worked up just as in the case of the quercetin derivative. 2-Hydroxy-4-ethoxy-ω: 6-dimethoxy acetophenone was obtained in an yield of 0·6 g.

Summary

Synthetic confirmation for the constitution of quercetagitrin is provided. The pentamethyl-quercetagetin obtained by the complete methylation and hydrolysis of the glucoside is finally ethylated and the product shown to be identical with a synthetic sample of 7-ethoxy-3: 5: 6: 3′: 4′-pentamethoxy

flavone (V) made from 2-hydroxy-4-ethoxy-ω: 6-dimethoxy-acetophenone (VI) using oxidation with persulphate, Allan-Robinson condensation and final methylation as stages. The ketone (VI) is conveniently made by the alkali fission of *O*-7-ethyl-3: 5: 3′: 4′-tetramethyl-quercetin obtained from quercimeritrin. This mixed ether of quercetin is also made independently by synthesis and this constitutes a synthetic confirmation of the constitution of quercimeritrin. Further, the transformations show the relationship between quercimeritrin and quercetagitrin as 7-glucosides. The most convenient synthetic route for the ketone (VI) is through the galangin derivative (XVI).

References

1. Rao and Seshadri .. *Proc. Ind. Acad. Sci.* A, 1941, **14**, 289.
2. ——— .. *Ibid*, 643.
3. Row and Seshadri .. *Ibid.*, 1945, **22**, 215.
4. ——— .. *Ibid.*, 1946, **23**, 140.
5. Attree and Perkin .. *J.C.S.*, 1927, 234.
6. Rao and Seshadri .. *Proc. Ind. Acad. Sci.*, A, 1939, **9**, 365.
7. Allan and Robinson .. *J.C.S.*, 1926, 2334.
8. Armstrong and Armstrong .. *The Glycosides*, p. 25.
9. Shibata and Hattori .. *Acta. Phytochem.*, 1930, **5**, 117.
10. Neelakantam, Rao and Seshadri .. *Proc. Ind. Acad. Sci.*, A, 1935, **1**, 887.
11. Kalff and Robinson .. *J.C.S.*, 1925, 181.

INFLUENCE OF TEMPERATURE ON THE RAMAN SPECTRA OF CRYSTALS

Part III. Barytes

By P. K. Narayanaswamy

(From the Department of Physics, Indian Institute of Science, Bangalore)

Received July 16, 1948

(Communicated by Sir C. V. Raman, Kt., F.R.S., N.L.)

1. Introduction

Although the Raman spectrum of barytes has been studied by a number of authors (Rasetti, 1932; Balakrishnan, 1941; Roopkishore, 1942; Krishnan, 1946 and others), its variation with temperature has not been investigated so far. In continuation of the work on calcite and quartz reported earlier in the *Proceedings* (Narayanaswamy, 1947 *a*, *b*) the author has now studied the influence of temperature on the Raman spectrum of barytes and the results are reported in this paper.

2. Experimental

A transparent piece of barytes ($1'' \times 1'' \times \frac{1}{2}''$) was used for these investigations. The experimental arrangements for obtaining the Raman spectra at different temperatures were the same as described in Part I of this series (Narayanaswamy, 1947 *a*). The spectra were excited by the λ 2536 resonance radiation of a quartz mercury arc and were photographed with a Hilger E3 medium quartz spectrograph. The variations in the position and width of the principal Raman lines were studied with the crystal held at 85, 300, 408, 513, 588, 698, 818 and 923° K. respectively. A fine slit 0·025 mm. wide was employed in order to obtain good resolution and exposures of the order of 3 hours were required to get reasonably intense spectrograms. With the large E1 spectrograph, two photographs, one with the crystal at room temperature and the other with the crystal held at 770° K. were taken in juxtaposition with the help of a Hartmann diaphragm to demonstrate clearly the effect of temperature on the various Raman lines.

3. Results

Typical spectrograms of the Raman spectrum of barytes with the crystal held at different temperatures are reproduced in Fig. 1 (Plate I). The E1 photograph is reproduced in Fig. 2 (Plate I). In Table I, the

measured frequency shifts of the principal Raman lines at various temperatures from that of liquid air to 923° K. are given. The total variation in their positions from room temperature to the highest attained, and the proportional change $\chi = 1/\nu.d\nu/dT$ for each of the important Raman lines are put down in Table II along with their measured widths at room temperature and at 923° K.

TABLE I

Variations in frequency shift of the principal Raman lines in barytes with temperature

$\nu_{85°K}$ in cm^{-1} liq. air temp.	$\nu_{300°}$ in cm^{-1} room temp.	$\nu_{403°}$ in cm^{-1}	$\nu_{513°}$ in cm^{-1}	$\nu_{588°}$ in cm^{-1}	$\nu_{638°}$ in cm^{-1}	$\nu_{818°}$ in cm^{-1}	$\nu_{923°}$ in cm^{-1}
75	74·5	74·2	73·1	71·7	71·5	71·0	69·5
90·2	89· 0	88·6	88·4	88·0	88·0	87·5	87·0
128·5	127·0	126·8	126·0	124·5	123·1	121·2	119·5
151·9	150	148·7	146·7	144·6	143·2	142·0	139·1
193	190	187·1	184	181·4	178·5	174·2	169·0
453	452·0	456	456	455·8	454	452·4	451
463·8	462						
648	647	644·1	643·2	642·6	641·5	642·5	641·2
991	989	986·3	983·0	981·4	979·1	976	972·0
1088	1084	1082	1079·5	1077·6	1074·3	1072	1067·0
1105	1104	1101·5	1098·5	1096·7	1094·0	1091	1087
1144·6	1142	1138·9	1136·4	1134·1	1130·6	1126·3	1121
1168·5	1.67	1165·5	1162	1159	1156·7	1152·4	1147·5

TABLE II

Total variations in frequency shift and width of the principal Raman lines and their proportional change χ

Centre of Raman line at 300°K. $\nu_{300°}$ in cm^{-1}	Centre of Raman line at 923°K. $\nu_{923°}$ in cm^{-1}	Shift $d\nu$ in cm^{-1}	Proportional change $\chi = 1/\nu.\frac{d\nu}{dT}$	Breadth of line at 300°K. in cm^{-1}	Breadth of line at 923°K. in cm^{-1}
74·5	69·5	4·9	$105·5 \times 10^{-6}$	4·2	8·0
89	87·0	2·0	36·1 ,,	5·2	8·5
127	119·5	7·5	95 ,,	4·1	12·0
150	139·1	10·9	116·7 ,,	5·0	12·5
190	169·0	21·0	177·4 ,,	5·9	20
452	451			5·2	36·1
462				8·2	
647	641·2	5·8	14·3 ,,	5·0	7·0
989	972·0	17·0	27·6 ,,	11·5	31·0
1084	1067	17·0	25·3 ,,	4·9	16·5
1104	1087	17·0	24·7 ,,	4·4	17·0
1142	1121	21·0	29·4 ,,	13·0	25·0
1167	1147·5	19·5	26·8 ,,	7·4	19·0

From Table I, it may be noticed that on cooling the crystal to liquid-air temperature, the Raman lines show an appreciable increase in frequency

shift. The increase is found to be greatest in the 190 cm.$^{-1}$ and the 1084 cm.$^{-1}$ Raman lines. That all the lines appear sharper at liquid air temperature will be evident from Fig. 1 (Plate I). With rising temperature, all the Raman lines shift more and more towards the exciting line. The extent of this diminution in frequency shift is, however, not the same for all the lines. For instance, when the temperature of the crystal is increased from

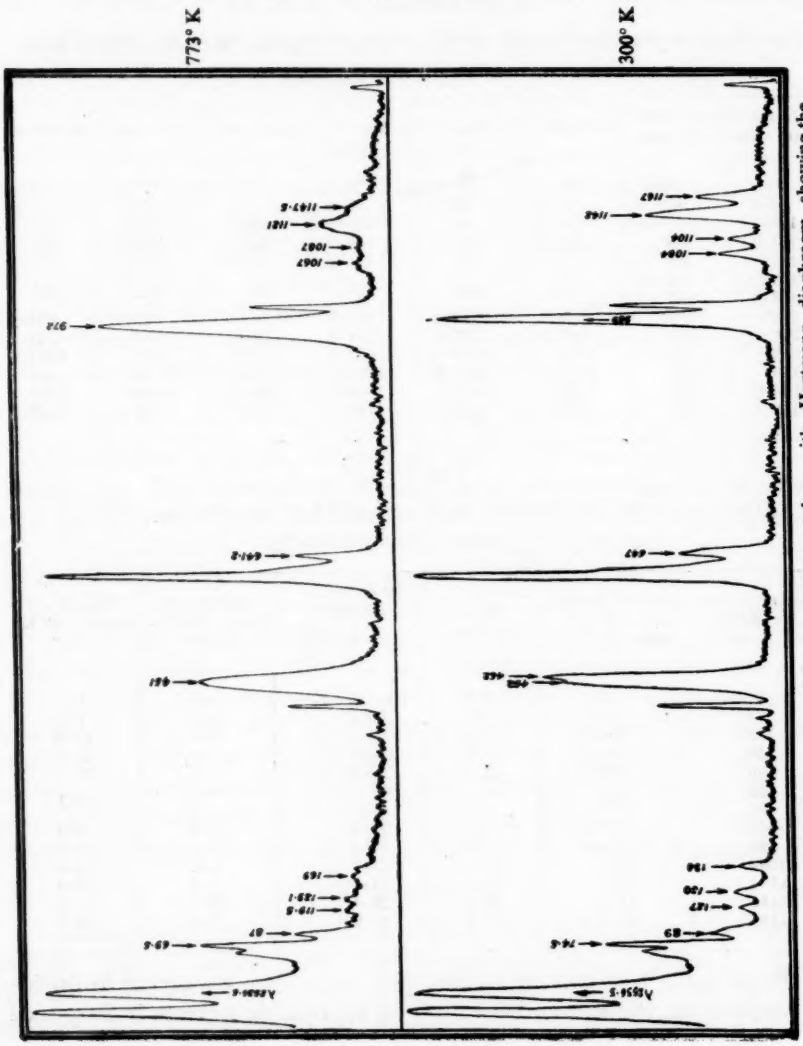

FIG. 3. Microphotometer curve of E1 spectrogram taken with Hartmann diaphragm, showing the variations in position and width of the principal Raman lines in barytes.

300° to 923° K., the 89 cm.$^{-1}$ Raman line shifts towards the exciting line by 2 cm.$^{-1}$ only, whereas for the same increase in temperature, the 190 cm.$^{-1}$ line shifts by about 20 cm.$^{-1}$ The internal frequencies also shift appreciably, the only exception being the 647 line which undergoes only a small shift. The total variations in the position and width of the different Raman lines can be seen vividly in the microphotometer curve of the E1 spectrogram reproduced in Fig. 3. The changes are also represented graphically for some of the important Raman lines in Fig. 4.

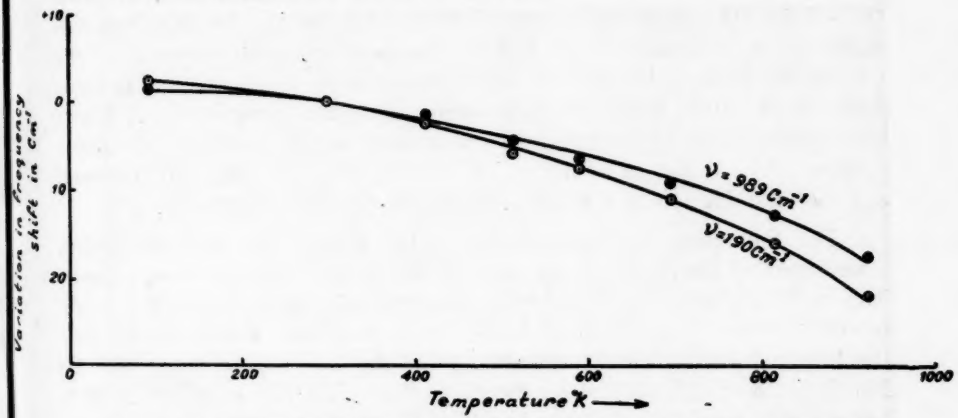

FIG. 4. Temperature dependence of the position of 190 cm.$^{-1}$ and 989 cm.$^{-1}$ Raman lines

It will be seen from Fig. 1 (Plate I) that as the temperature of the crystal is increased, the Raman lines broaden out considerably. This increase in the width of the lines is different for the various Raman lines. The lattice lines at 74·5 and 89 cm.$^{-1}$ for instance, remain appreciably sharp even at very high temperatures, while the other lattice lines broaden out greatly. The maximum increase in width is shown by the lattice line at 190 cm.$^{-1}$ and the internal frequencies at 989 and 1142 cm.$^{-1}$ The 647 cm.$^{-1}$ line exhibits the least amount of broadening. The 452–462 cm.$^{-1}$ doublet becomes a broad band as soon as the crystal attains temperatures higher than the room temperature. At very high temperatures, the lattice lines at 127 and 150 cm.$^{-1}$ as also the 1084 and 1104 cm.$^{-1}$ lines merge into one another. The 1167 cm.$^{-1}$ Raman line becomes very diffuse at high temperatures.

4. DISCUSSION

Spectrum of the SO_4 ion.—In the free state, the SO_4 ion has only 4 distinct modes of vibration whose frequency shifts are 454 (2), 622 (3), 983 (1) and 1106 (3) cm.$^{-1}$, the figures in brackets being their respective

degeneracies. At room temperature, with the disappearance of degeneracy, the spectrum of barytes crystal shows actually 11 frequency shifts attributable to the SO_4 group, 9 of which are due to the splitting up of the 4 distinct modes of oscillation characteristic of the SO_4 ion into components in the crystal and the remaining two arise from the Fermi splitting of two of the fundamental frequencies (Krishnan, *loc. cit.*). With rising temperature of the crystal, however, it is observed that the 452 and 462 cm.$^{-1}$ lines which are the two components into which the 454 (2) fundamental mode of oscillation of the SO_4 group splits, merge into one another and become indistinguishable as separate entities. Similar tendencies are also observed in the case of the 1094, 1142 and 1167 cm.$^{-1}$ Raman lines which are the components of the 1106 (3) fundamental mode, at higher temperatures. These observations tempt us to remark that with increasing temperature, the degeneracies of the modes of oscillation of the SO_4 group are gradually restored and the vibrating ion as a whole tends to attain greater symmetry.

The diminution in frequency shift of the Raman line with increasing temperature of the crystal is not uniform for equal changes in temperature. This will be clear if we consider the proportional change, χ *i.e.*, $1/\nu \cdot d\nu/dT$ for the different ranges of temperature for each of the Raman lines. For the 150 cm.$^{-1}$ lattice line for example, χ for the temperature range 85° to 300° K. is 58×10^{-6} whereas for the range 698° to 923° K. it is 127×10^{-6}. For the 1067 cm.$^{-1}$ line, the values are 6×10^{-6} and 35×10^{-6} for the same ranges of temperature. It will be seen that the proportional change is greater at high temperatures than at low temperatures, the value of χ increasing with rising temperature. This is clearly shown in Fig. 4 where the temperature frequency shift curve exhibits a greater slope at higher temperatures, and tends to flatten at low temperatures although it does not actually become so.

The mean χ values for the various Raman lines for the temperature range 300–923° K. are given in Table II. The value of χ ranges from $14{\cdot}3 \times 10^{-6}$ to $177{\cdot}4 \times 10^{-6}$. It will be easily seen that χ for the different lattice lines is of the same order of magnitude indicating that the lattice forces are temperature sensitive to more or less the same extent. The only exception is the 89 cm.$^{-1}$ line which shows a very low temperature sensitivity. The different internal frequencies also have χ values which are of the same order of magnitude, *i.e.*, about 25×10^{-6} which shows that the internal oscillations of the SO_4 ion are affected to nearly the same extent by temperature variations. Here again, the 647 cm.$^{-1}$ line shows a very low temperature sensitivity. As was observed in the case of calcite by the author (*loc. cit.*), the lattice frequencies exhibit greater χ values than the internal frequencies, showing that the former are much more temperature sensitive than the latter.

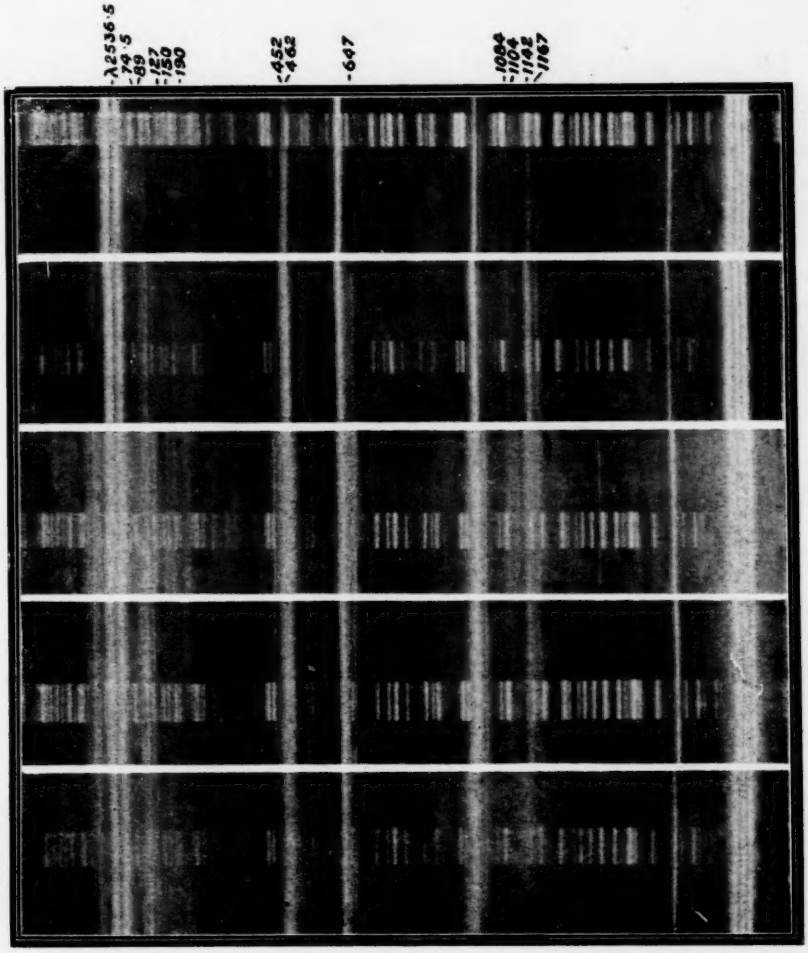

FIG. 1. Raman spectrum of barytes at various temperatures taken with E 3 spectrograph

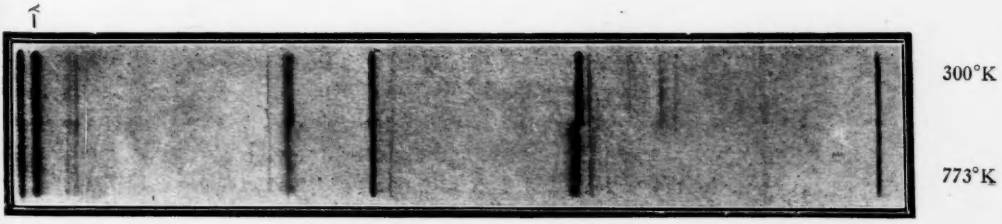

FIG. 2. Raman spectrum of barytes taken with E 1 spectrograph using Hartmann diaphragm

Regarding the width of the Raman lines, it is interesting to observe that those lines which do not show appreciable temperature variations in frequency shift like the 89 and 647 cm.$^{-1}$ Raman lines, do not also broaden out perceptibly. These lines remain sharp even at very high temperatures, whereas the lines which broaden out enormously, *e.g.*, 190 and 989 cm.$^{-1}$ Raman lines, also show considerable diminution in frequency shift, the variations in position and width being of comparable order of magnitude. The increase in width is, however, greater in all cases than the decrease in frequency shift. These observations tend to support the idea that the diminution in frequency shift and the increase in width of the Raman lines observed in crystals with rising temperature are closely connected and interrelated, as indicated by Sir C. V. Raman (1947). It may be also remarked that the peak intensity of the different Raman lines undergoes a notable diminution with increasing temperature (see Fig. 3).

In conclusion, the author wishes to express his heartfelt thanks to Prof. Sir C. V. Raman, Kt., F.R.S., N.L., for his keen interest and inspiring guidance in the course of this investigation.

Summary

The Raman spectrum of barytes excited by the λ 2536 radiation of the mercury arc has been studied at a series of eight temperatures ranging from 85° to 923° K., and data furnished regarding the variations in frequency shift and the width of the principal Raman lines. With increasing temperature a definite decrease in frequency shift is observed, the rate of decrease being greater at higher temperatures. While at low temperatures the internal frequencies of the SO_4 ion are clearly split up into distinct components, these tend to coalesce as the temperature is increased. The lattice oscillations are observed to be much more temperature sensitive than the internal oscillations of the SO_4 group. The 89 cm.$^{-1}$ lattice line and the 648 cm.$^{-1}$ internal frequency are comparatively the least affected by temperature variations.

References

1. Rasetti .. *Nuovo Cimento*, 1932, **9**, 72.
2. Balakrishnan, T. A. S. .. *Proc. Ind. Acad. Sci.*, A, 1941, **14**, 257.
3. Roopkishore .. *Ibid.*, 1942, **16**, 36.
4. Krishnan, R. S. .. *Ibid.*, 1946, **23**, 288.
5. Raman, Sir C. V. .. *Ibid.*, 1947, **26**, 339.

6*a*. Narayanaswamy, P. K. .. *Ibid.*, 1947, **26**, 511.

b. ———— .. *Ibid.*, 1947, **26**, 521.

EFFECT OF DUST AND HAZE ON THE SPECTRAL DISTRIBUTION OF ZENITH-SCATTERED RADIATION

By R. V. Karandikar, M.Sc.

Received June 12, 1948
(Communicated by Dr. K. R. Ramanathan, M.A., D.Sc., F.A.Sc.)

1. Introduction

Observations of the light scattered from the zenith sky made with Dobson's photoelectric spectrophotometer at Jackko, Simla, in April and May 1947 showed that there were certain well marked differences in the intensity-ratios I''/I' and I'/I as measured on clear and hazy days. Here I, I′, I″ are the intensities of the three wavelengths λ (3110 A), λ' (3300 A) and λ'' (4450 A) respectively, λ being strongly absorbed by the atmospheric ozone, λ' only slightly and λ'' not at all. Log I''/I' when plotted against the zenith distance Z of the sun was found to be markedly higher on hazy days than on clear days. It was further noticed that on hazy days, as Z decreased from 90° to 0°, log I''/I' had first a rapid decrease, but that later, when Z was near about 45°, its value reached a minimum. It again rapidly increased when Z was less than 20°. Calculations of primary molecular scattering showed that the curve should have continued decreasing with Z right down to $Z = 0$. These deviations from the calculated curve became less marked on days with less haze but were evident even on days of apparently very clear skies.

This peculiarity of the variations of zenith sky light for small zenith distances of the sun can naturally be better observed in low latitudes where high suns are frequent. The present paper gives the results of zenith sky observations obtained on a number of hazy and clear days at Simla and Delhi and discusses the origin of the above phenomenon as due to scattering by large particles.

2. Observational Data

Dobson's spectrophotometer directly measures the values of log I''/I' and log I/I' for the two pairs of wavelengths in the light scattered from the zenith sky. Since the variations of the two quantities with the zenith distance Z of the sun are in opposite directions, for convenience of comparison, the reciprocal quantity log I'/I instead of log I/I' is used hereafter and the instrumental constants to be added to log I''/I' and log I'/I are also dropped out.

The skies at Simla (2·45 km. a.s.l.) are generally clear up to the middle of April, but later the duststorms of the North Indian plains frequently raise dust above the height of Simla. Observations were carried out both on clear cloudless days and on days of different degrees of haziness in April and May, 1947. Due to disturbed political conditions in the country, observations at Simla could again be started only in the month of November, 1947. The skies in the winter series of observations were much clearer than in the hot season, but the lowest zenith distance of the sun obtained in the winter series was only 47° as against 13° in the summer.

Fig. 1 gives the plots of log I″/I′ and log I′/I against the zenith distance Z of the sun measured from sunrise to sunset on a few days at Simla.

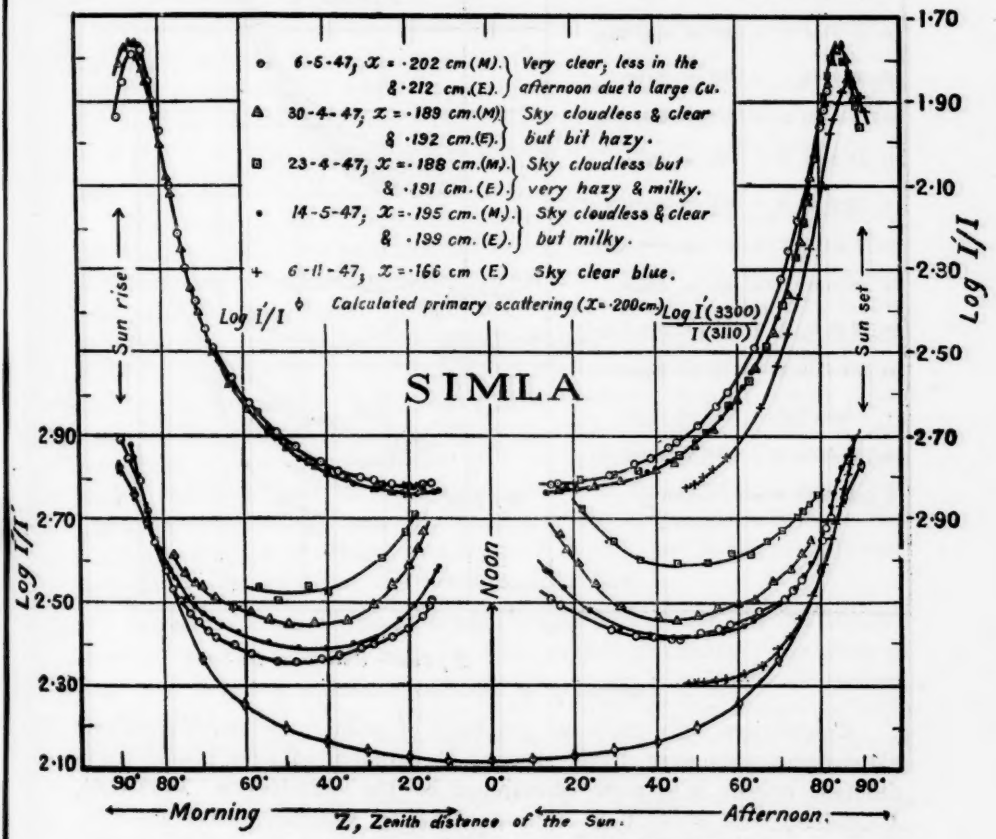
6-5-47, χ = ·202 cm (M). & ·212 cm. (E). Very clear; less in the afternoon due to large Cu.
30-4-47, χ = ·189 cm. (M) & ·192 cm. (E). Sky cloudless & clear but bit hazy.
23-4-47, χ = ·188 cm. (M). & ·191 cm. (E). Sky cloudless but very hazy & milky.
14-5-47, χ = ·195 cm. (M). & ·199 cm. (E). Sky cloudless & clear but milky.
6-11-47, χ = ·166 cm (E) Sky clear blue.
Calculated primary scattering (χ = ·200 cm)
Log I′/I
Log I′(3300)/I(3110)
Sun rise
Sun set
SIMLA
Noon
Morning
Afternoon
Z, Zenith distance of the Sun.
1·70
1·90
2·10
2·30
2·50
2·70
2·90
90° 80° 60° 40° 20° 0° 20° 40° 60° 80° 90°

FIG. 1. Observations of zenith sky radiation at Simla

The ozone amounts and sky conditions are also indicated. Fig. 2 gives similar data obtained for Delhi. Though the sky haziness observed at Delhi was much more varied than at Simla, complete curves for Delhi from midday to sunset or sunrise were available on very few occasions. Only the later more complete observations at Simla revealed the usefulness of taking complete series of observations to explain the phenomenon.

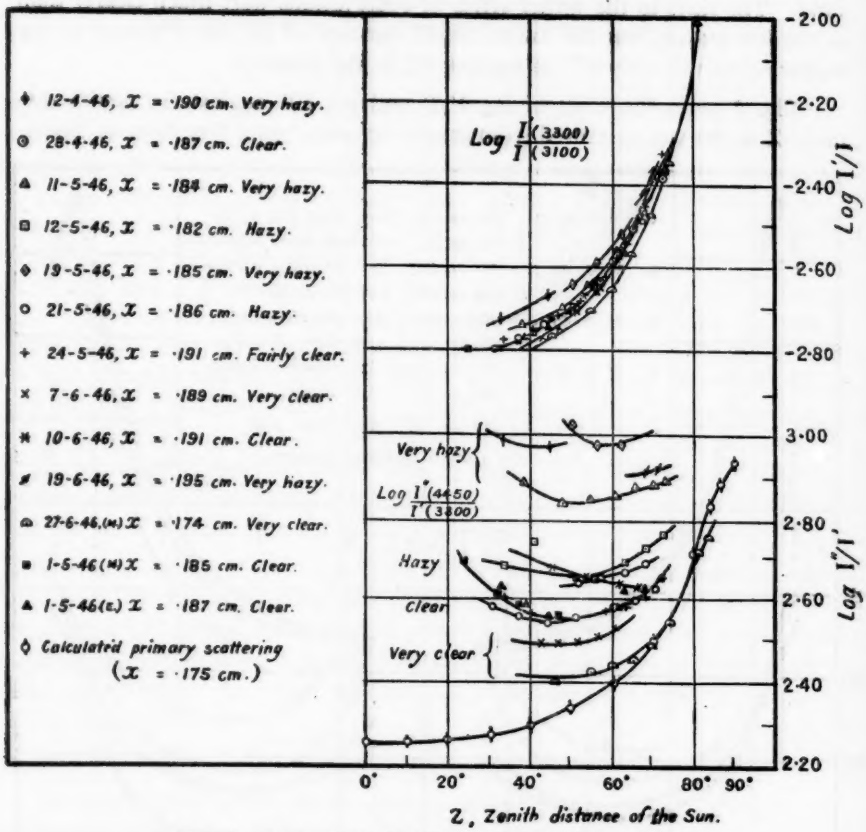

FIG. 2. Observations of zenith sky radiation at Delhi

Calculations were made on the basis of primary molecular scattering alone and curves were drawn showing the amount of light coming from different heights in a pure atmosphere at the wavelengths λ (3110 A), λ' (3300 A) and λ'' (4450 A) corresponding to assumed ozone amounts. The ratios I''/I' and I'/I for the integrated intensities were calculated from these and these calculated curves are also shown in Figs. 1 and 2.

3. Variation of the Intensity Ratios with the Degree of Haziness of the Sky

Since molecular scattering, ozone absorption and particle scattering affect the three wavelengths differently, the two ratios I″/I′ and I′/I would show corresponding differences. Observations show that the ratio for the longer wavelengths is much more susceptible to changes in haziness of the sky than that for the shorter wavelengths. Calculation also shows that changes in log I″/I′ due to the variations in ozone amounts found on the different days of observation are negligible. As the wavelength interval $\lambda''-\lambda'$ between 4450 and 3300 A is much larger than the interval $\lambda'-\lambda$ between 3300 and 3110 A, the effect of haze scattering on log I″/I′ may be expected to be much larger than that on log I′/I.

The upper curves of log I′/I in Figs. 1 and 2 show that (1) with increasing ozone amount, the intensity in the shorter wavelength decreases at all zenith distances and (2) when the ozone amount remains the same but the sky haziness increases, the ratio log I′/I is not appreciably altered at angles of $Z > 45°$ but that at lower angles there is a small but appreciable rise in the curve when the sky is very hazy.

The curves of log I″/I′ show much greater diversity. The lowest curve in the afternoon refers to a very clear day with the least ozone amount 0·166 cm. and the lowest curve in the morning to a clear day with the highest ozone amount 0·202 cm. Higher up there are curves relating to days with nearly the same ozone amount but with different degrees of haziness. It is obvious that sky haze affects the long wavelength curves much more than the ozone amount, increasing haze increasing the relative intensities in the longer wavelength. Thus clearest days in winter show the lowest values of log I″/I′ and very hazy days in the hot season give the highest values; days of intermediate haziness show intermediate values. Since the curves sort themselves out in the order of haziness, the elevation of the curve above the molecular scattering curve at some specified angle—$Z = 45°$ near the minimum is very convenient—can be taken as a measure of the haze.

We can also get a measure of atmospheric haze or turbidity in a different way. It was pointed out in a previous paper[1] discussing 'the effect of dust and haze on direct sun observations made with Dobson's spectrophotometer' that the quantity $\delta'-\delta'' = (L'-L'_0)/m - \alpha' x - (\beta_1'-\beta_1'')$ obtained from direct sun observations would be a convenient measure of atmospheric turbidity. To try this out, the values of log I″/I′ at $Z = 45°$ were plotted against the mean values of $(\delta'-\delta'')$ obtained from direct sun observations made at the same time. Fig. 3 shows these plots separately

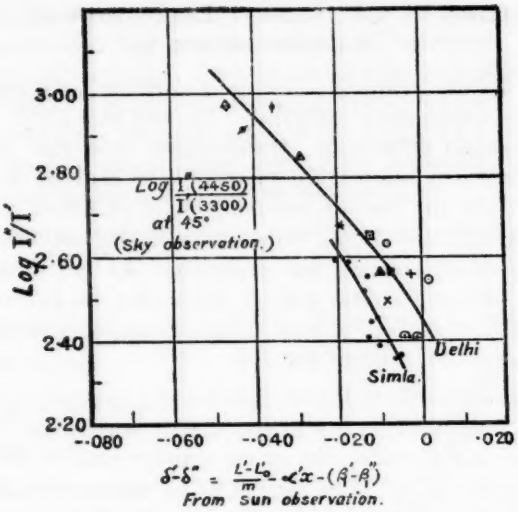

FIG. 3. Atmospheric haze from zenith sky intensity and direct sun observations

for Simla and Delhi. It is seen that log I″/I′ increases more or less regularly with increase in the numerical value of $(\delta'-\delta'')$. Unfortunately all the observations presented here are those in the summer and the sign of $(\delta'-\delta'')$ remains negative throughout this period. The numerical value of $(\delta'-\delta'')$, however, increases with increase in haziness. The observational points for the two places Simla and Delhi show that there is a definite correlation between the value of the ratio log I″/I′ and the amount of haze in the atmosphere. The lateral shift of the Simla curve with respect to the Delhi curve on the side of larger numerical values of $(\delta'-\delta'')$ is not significant, as the value of the constant to be added to log I″/I′ at the two places is different.

The reason why log I″/I′ increases with increase in the haziness of the sky is obvious. In an ideally clear atmosphere, the scattering is selective and there is predominance of shorter wavelengths in the scattered light, the variation being according to Rayleigh's inverse fourth power law. Any increase of large-sized scattering material in the sky would mean an addition of scattered radiation for which the value of n in the scattering law λ^{-n} would be smaller than 4. The ratio I″/I′ will therefore increase. With increase in the size of the haze particles, the scattered radiation will increase in quantity and become richer in longer wavelengths. For very large particles, however, the scattering becomes non-selective and the ratio I″/I′ would remain practically unaffected.

4. Variation of the Intensity Ratios with the Zenith Distance of the Sun

Apart from the above-mentioned general increase in the values of log I″/I′ with increase in the haziness of the sky, another very interesting fact is that log I″/I′ shows a minimum near about 45° and a rapid *increase* in value for values of Z less than 20°. The curve of log I′/I also shows a similar but much feebler rise for low values of Z. Calculations of primary molecular scattering show that the curve should steadily decrease and be horizontal near Z = 0. The deviations from the calculated curves become less marked on clear days but are quite evident even on days of apparently very clear skies.

The peculiar rise in the curves of log I″/I′ for values of $Z < 45°$ can perhaps be better understood by decomposing the observed curve into the molecular scattering curve and the curve of residue, *viz.*, the difference between the observed and calculated curves. Fig. 4 shows the observed curves, the calculated curves and the residual curves for two days of different degrees of haziness at Simla. The observed curve can be considered to be the resultant of the molecular scattering curve and the residual curve. This residue curve gives the contribution due to large particle scattering.

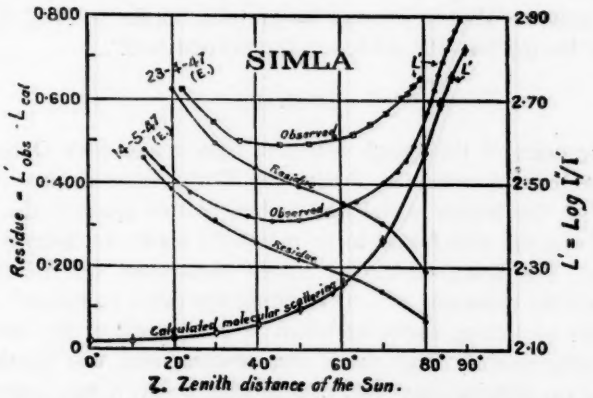

Fig. 4. Resolution of zenith sky intensities into molecular and large particle scattering intensities—at Simla

5. General Remarks

It is well known from the work of Mie,[2] Lord Rayleigh,[3] Blumer,[4] Stratton and Houghton,[5] Sinclair[6] and others that the scattering of light by transparent spherical particles which are not small in size compared with the wavelength of light differs from the scattering by small particles in the following important respects.

(1) The scattering cross-section S is a function of $2\pi r/\lambda$. It is very small for values of $2\pi r/\lambda < 0{\cdot}5$ but increases rapidly with increase of $2\pi r/\lambda$, reaching a maximum at a value which depends on the refractive index of the particles, then goes down to a minimum, again reaches a feebler secondary maximum and ultimately reaches a value equal to $2\pi r^2$ for large values of $2\pi r/\lambda$. For particles of refractive index 1·33, the first maximum is reached when $2\pi r/\lambda$ is nearly 6 and the first minimum when it is nearly 11.

(2) A large fraction of the total scattered light by large particles is concentrated in a small cone about the direction of the incident light. The larger the value of r/λ, the smaller is the angle of the cone within which half the total scattered light is concentrated. For example, for wavelengths with $2\pi r/\lambda$ equal to 160, half the light lies within a cone of semi-vertical angle 7°.

The detailed analysis of scattering by atmospheric haze is very complicated, because the atmosphere contains particles of many sizes and the incident light is composed of many wavelengths. Moreover, the particles are not concentrated in a thin layer but are spread out in depth so that secondary and multiple scattering becomes important and detailed calculation becomes exceedingly difficult.

The author wishes to express his grateful thanks to Prof. K. R. Ramanathan for his interest and advice in the present work.

Summary

Observations of the zenith scattered light made with Dobson's photoelectric spectrophotometer at Simla and Delhi showed that the intensity ratio I″/I′ for the longer wavelengths when plotted against the zenith distance Z of the sun was found to be markedly higher on hazy days than on clear days. The observed curves sorted themselves out in the order of haziness and the elevation of a curve above the curve calculated on the basis of molecular scattering could be taken as a measure of the haze. $(\delta'-\delta'')$, obtained independently from direct sun observations, was another measure of haze and on plotting these two against each other, it was found that there was clear correlation between them.

Another interesting fact observed was that as Z decreased from 90° to 0°, log I″/I′ had first a rapid decrease, showed a minimum near about 45° and for still lower values of Z showed an *increase*, the increase being rapid below 20°. Calculations of primary molecular scattering showed that the curve should steadily decrease with Z right down to Z = 0°. These deviations from the calculated curve became less marked on clear days but were

quite evident even with apparently very clear skies. On decomposing the observed curve into the molecular scattering curve and the curve of residue, it was seen that this residue curve indicated very large intensities at small angles from the direction of incidence, decreasing rapidly as the angle increased and could be reasonably attributed to scattering by large particles present in the atmosphere.

References

1. K. R. Ramanathan and R. V. Karandikar .. "Effect of dust and haze on direct sun observations made with Dobson's spectrophotometer." In course of publication.
2. G. Mie .. *Ann. der Phys.*, 1908, **25**, 377.
3. Lord Rayleigh .. *Scientific Papers*, 1899, Vol. I, p. 92; Vol. IV, p. 400.
4. H. Blumer .. *Zeit. für Phys.*, 1925, **32**, 119; 1926, **38**, 304; 1926, **38**, 920; 1926, **39**, 195.
5. Stratton and Houghton .. *Phy. Rev.*, 1931, **38**, 159.
6. D. Sinclair .. *Jour. Opt. Soc. of America*, 1947, **37**, 475.

DIFFRACTION OF LIGHT BY VERY HIGH FREQUENCY ULTRASONIC WAVES: EFFECT OF TILTING THE WAVE FRONT

By S. Bhagavantam, F.A.Sc., and B. Ramachandra Rao
(From the Department of Physics, Andhra University, Waltair)

Received July 1, 1948

1. Introduction

Asymmetry in the diffraction spectra produced by a tilt in the sound wave front from the position of normal incidence was observed by Debye and Sears[1] and by Lucas and Biquard.[2] The diffraction spectrum of the mth order attains its maximum intensity for a tilt angle given by

$$\theta = \sin^{-1} m\lambda / 2\mu_0 \cdot \lambda^*, \qquad (1)$$

where μ_0 is the refractive index of the medium, λ is the wave length of light in vacuum and λ^* is the wave length of sound in the medium. Detailed investigations were made later by Bär[3] and Parthasarathy.[4] Photographs obtained by Bar showed the asymmetry introduced on tilting the sound wave front through an angle of $< 1°$. For a truly normal incidence, a symmetrical diffraction picture and for oblique incidence, a picture with more orders on one side than on the other were obtained. Parthasarathy used progressive sound waves set up in a 12″ column of benzene at a frequency of 7·37 Mcs/sec. and measured the tilt angles in a rough way by attaching a rigid steel rod of 31 cm. to the crystal holder and observing the readings of its end on a vertical scale. Tilting the sound wave front from the normal incidence position, greatest asymmetry in the diffraction spectrum was noticed at an angle of 22′. When the angle of incidence was further increased, the number of diffraction images was found to decrease, and finally disappear almost completely at about 2°. Using a frequency of 20 Mcs./sec., Parthasarathy[5] later showed that intense diffraction spectra on one side of the central image could be obtained for certain angles of incidence given by the Bragg relation. Rytov[6] investigated the effect of tilting the sound wave front on diffraction, both theoretically and experimentally, in the range of 30 to 70 Mcs. His observations showed that at these frequencies, the intensity distribution approximated closely to selective reflection at the Bragg glancing angle. Quantitative measurements of the intensity of first order diffracted light in air for varying angles of incidence were made by Korff.[7] The ratios of the intensities of the first order to the central order

were estimated on a microphotometer and compared with the theory of Brillouin. A maximum of diffracted light was found at the Bragg angle of incidence.

The highest frequency at which diffraction effect has so far been studied is thus only 70 Mcs./sec. and this was by Rytov. During the past few years, we have been studying the different aspects of diffraction by very high frequency ultrasonic waves and we have succeeded in generating and using sound waves of frequencies upto 200 Mcs./sec. for this purpose. In this investigation, the effects produced by tilting the wave front are described in some detail.

2. Experimental Details

Four different frequencies, namely, 25, 50·36, 102·6 and 177·2 Mcs./sec. have been used. The wave-length of sound in water corresponding to the highest frequency used here is 0·000849 cm. This is only about 14 times the wave-length of sodium yellow light, which is generally employed by us for obtaining the patterns. The oscillators for generating the 177·2 and 102·6 Mcs. radio waves are specially designed and constructed using a T-55 valve. The circuit for the 50 Mcs. oscillator is the same as that used for 100 Mcs. with slight modifications. A coil of 2″ diameter containing two turns of thick tinned copper wire serves as the tank circuit inductance. A Meissner R. F. choke of 2·5 mH with a current carrying capacity of 250 mA is used in the plate circuit. The crystal is connected to a coil of about four turns of copper wire mounted on an amphenol insulator. By varying the distance of this coil from the tank coil of the oscillator the power input to the crystal can be altered. The 25 Mcs. oscillator is of the regular Hartley type using 815 valve and is also coupled to the crystal by a mutual inductance coil, again enabling us to vary the power of excitation of the crystal.

The arrangement for observing and recording the diffraction patterns is the usual one with slight modifications. Water is the medium in which all the effects described in this paper have been studied and 6 mm. square apertures are introduced in the light emerging from the collimator to get uniform light intensity with square cross-section. Except for the low frequency of 25 Mcs., for all the other frequencies a 3″ glass cell is found to be sufficient for producing progressive waves, the absorption coefficient then being sufficiently high that the wave gets completely damped before touching the bottom of the cell. For the 25 Mcs. ultrasonic wave, however, a 12″ height of glass cell stuffed with glass wool and felt padding at the bottom is used for getting a truly progressive sound wave. Any deviation from the truly progressive nature of the wave can be detected by tilting the cell in a

plane at right angles to the direction of the light beam. If any change in the intensity of the diffracted light is noticed it can be taken as an indication that the wave is not a pure progressive wave. This test is necessary and must be applied only when the light beam is incident normally on the faces of the glass cell.

A mirror is rigidly attached to the crystal holder and a telescope and scale placed at a distance of about one metre are used to note the position of the crystal holder. The direction of observation through the telescope is set almost parallel to the direction of the light beam. With this arrangement, very slight variations in the tilting of the crystal holder can be easily detected.

3. Results

Starting from the normal incidence position of the sound wave front, the crystal holder is tilted through known angles and the intensities of both the first order diffraction lines are visually estimated. For all the four frequencies of the sound waves, the maximum intensity of the first order diffraction line is adjusted to be approximately the same and the effect of tilt studied. Visual estimates of the intensities of + 1 and − 1 orders for different angles of tilt θ from the normal incidence position are given in Table I. Table II gives the angles through which the crystal has to be tilted

Table I

25 Mcs. ..	θ	−18′		−11·5′	−6′	−4·5′	0	4·5′	6′	11·5′	18′	
	I_{+1}	0		0	0	0	3	8	10	20	12	
	I_{-1}	12		20	10	8	3	0	0	0	0	
50·36 Mcs. ..	θ	−32′	−26′	−21′	−16′	−3′	0	3′	16′	21′	26′	32′
	I_{+1}	0	0	0	0	0	1	1·5	6	10	20	8
	I_{-1}	8	20	10	4	1·5	1	0	0	0	0	0
100·26 Mcs. ..	θ	−56′	−52′	−50′	−46′	−43′	0	43′	46′	50′	52′	56′
	I_{+1}	0	0	0	0	0	0	2	4	10	20	4
	I_{-1}	4	20	10	4	2	0	0	0	0	0	0
177·2 Mcs. ..	θ	−89′		−88′	−84′	0		84′		88′	89′	
	I_{+1}	0		0	0	0		1		10	20	
	I_{-1}	20		10	1	0		0		0	0	

Table II

Frequency of sound in Mcs./sec.	θ Calculated	θ Measured
25	12·7′	11·5′
50·36 (+1)	25·5′	26′
(+2)	51′	52′
102·6	51·4′	52′
177·2	90′	89′

from the normal incidence position to get a maximum intensity for the first order. This angle is compared with the angles computed from formula (1). With increased power input, even the second order at 50 Mcs. could be obtained, but only at the proper inclination and the observed angle compared well with that calculated from the formula. In Table III, the value given in the columns designated by $\phi\frac{1}{3}$ and $\phi\frac{1}{2}$ represents the fraction, with reference to the Bragg reflection angle in each case, of the sound wave front tilt from the maximum intensity position required to reduce its intensity to $\frac{1}{2}$ and $\frac{1}{3}$ respectively. ϕ_0 stands for the tilt angle, similarly expressed as a fraction, at which the disappearance of the order takes place. This table brings out the increasing sharpness of the phenomenon with increasing frequency of sound waves.

TABLE III

	25	50	102	177 Mcs.
$\phi\frac{1}{2}$ ..	1/2	1/5	1/26	1/90
$\phi\frac{1}{3}$ ..	2/3	1/3	1/13	1/50
ϕ_0 ..	4/3	9/8	1/4	1/11

The estimates of intensities are plotted in Fig. 1. For the lower frequencies of 25 and 50 Mcs., both I_{+1} and I_{-1} are plotted, while for the two higher frequencies, only I_{+1} is given.

The special features observed in the case of very high frequencies are summarised below.

(*a*) It has not been possible to get the second or higher orders in the diffraction patterns. This is in sharp contrast with the observations at low frequencies where the second and higher orders are easily excited with moderate power.

(*b*) The first order diffraction line appears with maximum intensity not for normal incidence but when the light rays meet the sound wave front at the Bragg angle of reflection. In this position, only a single diffraction line on the appropriate side is obtained, the diffraction line on the other side of the central image having completely disappeared. In no position has it been possible to get both the first order lines on either side of the centre at the same time.

(*c*) The value of the angle for which the first order line attains its maximum intensity is quite critical. Fig. 1 shows that a slight tilt of the crystal holder, about 2′ for the 102 Mcs. and 1′ for the 177 Mcs., will reduce the intensity of the diffraction order by half. Contrary to this, the behaviour

of diffraction at 50 and 25 Mcs. shows that in this region the range of reflection is not sharp. Tilting the crystal by 13 for the 100 Mcs. and 8′ for the

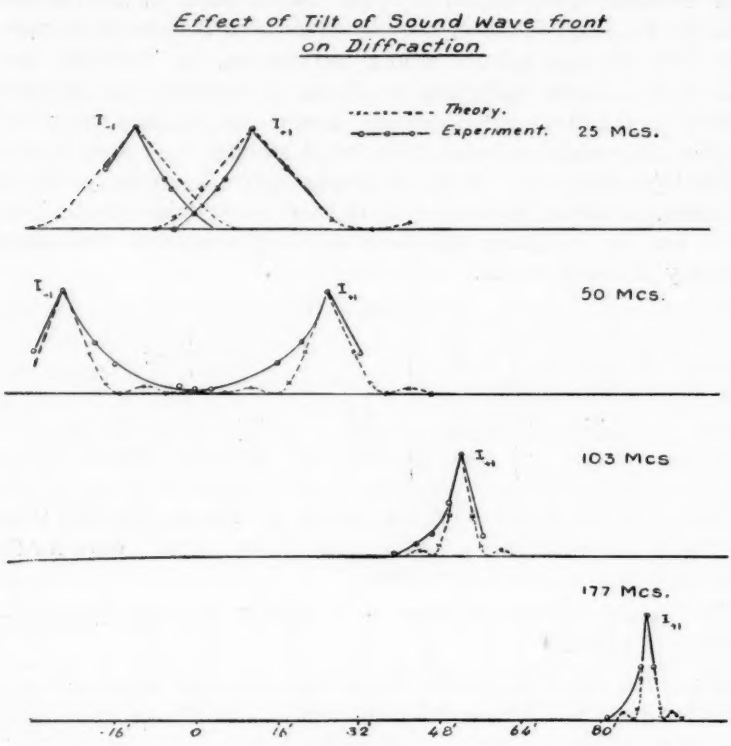

FIG. 1

177 Mcs. from the maximum intensity position of the first order, makes the diffraction effect completely disappear. Thus for normal incidence, no diffraction lines are obtained at these frequencies whereas for 25 and 50 Mcs., at normal incidence the first order lines on both the sides of the central image are obtained symmetrically though with less intensity. The disappearance of diffraction for normal incidence for the very high frequencies shows that the diffraction of light in the ordinary sense does not exist in this region. On the other hand, the reflection phenomenon predicted by Brillouin becomes conspicuous.

4. COMPARISON WITH THEORY

Raman and Nath[8] have given a generalised theory of diffraction in which was obtained a difference-differential equation whose solutions correspond

to the amplitudes of the diffraction orders. Nath[9] has solved the difference-differential equation by the series method and has shown that the maxima of intensity of first and second orders of diffraction occur at angles of $\lambda/2\mu_0\lambda^*$ and $\lambda/\mu_0\lambda^*$ under certain conditions. This result is in agreement with our observations. An attempt to calculate the intensities using the expressions given by Nath with suitable parameters has not been successful as it is found that the series is not convergent. In the same paper Nath has suggested a method of determining the amplitude of the fluctuation of the refractive index at high supersonic frequencies by determining the ratio of the intensities of central to the first order for normal incidence and + 1 to − 1 order for oblique incidence. Such observations are not possible at the very high frequencies used by us since both the diffraction orders are never present at the same time.

Following the procedure adopted by Brillouin, expressions for intensities of first and second orders of diffraction have been deduced by David,[10] on the assumption that the higher orders are of negligible intensity. To a first approximation the following expression is obtained for I_{+1}, the fraction of the intensity of the first order to the total incident light.

$$I_{+1} = \left(\delta \frac{\sin (\alpha - \frac{1}{2})\, \bar{x}_0}{(\alpha - \frac{1}{2})}\right)^2 \tag{2}$$

where $\delta = \mu\mu_0 \lambda^{*2}/\lambda^2$

$\alpha = \mu_0\lambda^*\theta/\lambda$

and $\bar{x}_0 = \pi\lambda L/\mu_0\lambda^{*2}$.

L is the length of the sound field traversed by light and θ is the inclination of the sound wave front. It can be easily seen that this expression attains its maximum intensity when $\alpha = \frac{1}{2}$ or $\theta = \lambda/2\mu_0\lambda^*$. This result is the same as (1) and is in agreement with the experimental observations. The maximum value of I_{+1} denoted by I_m comes out as

$$I_m = \delta^2 \bar{x}_0^2$$

$$= \frac{\pi^2\mu^2 L^2}{\lambda^2} = \frac{1}{4}\left(\frac{2\pi\mu L}{\lambda}\right)^2 \tag{3}$$

Using I_m given by equation (3), we get the expression (2) modified as

$$I_{+1} = I_m\left(\frac{\sin (\alpha - \frac{1}{2})\, \bar{x}_0}{(\alpha - \frac{1}{2})\, \bar{x}_0}\right)^2. \tag{4}$$

Substituting

$$\theta = \frac{\lambda}{2\mu_0\lambda^*} + \phi,$$

where ϕ is the deviation of the sound wave front from the maximum intensity position of the first order, we get

$$\bar{x}_0 (a - \tfrac{1}{2}) = \frac{\pi L \phi}{\lambda^*}.$$

The expression for the intensity of the first order becomes

$$I_{+1} = I_m \left(\frac{\sin \frac{\pi L \phi}{\lambda^*}}{\frac{\pi L \phi}{\lambda^*}} \right)^2. \tag{5}$$

This relation is extremely important and contains many noteworthy features which are supported by experiment. These features are described below in some detail. The intensity of a particular order will vanish whenever $L\phi/\lambda^*$ is an integer other than zero. Thus, there are three ways of making a diffraction line periodically vanish. The first is by making the tilt angle ϕ of the sound wave front take successively the values λ^*/L, $2\lambda^*/L$ and so on. This phenomenon was experimentally observed by Debye and Sears and a simple explanation was given by Raman and Nath. The second is by making the sound field length L take successively the values λ^*/ϕ, $2\lambda^*/\phi$ and so on. This phenomenon has not been observed so far by any of the investigators. Korff[7] studied the dependence of intensity on the length of the sound field but his results show only a tendency towards decreasing intensity with increasing length at a certain stage but do not show a passage through successive minima. Such a passage through successive minima has been observed by us using a specially large-sized crystal and results which are in agreement with the above theory obtained. These will be described in a separate communication. The third method is to make λ^* take successively the values $L\phi$, $L\phi/2$ and so on. No one appears to have worked on these lines. For normal incidence, ϕ in respect of the first order line is equal to θ given by (1) with $m = 1$ and substituting this value in (5), we have

$$I_{+1} = I_m \left(\frac{\sin \frac{\pi L \lambda}{2\mu_0 \lambda^{*2}}}{\frac{\pi L \lambda}{2\mu_0 \lambda^{*2}}} \right)^2.$$

As the numerator in the bracket is always less than 1, we cannot have even the first order line appearing with appreciable intensity in normal incidence if $\pi L\lambda/2\mu_0\lambda^{*2} >> 1$. This is equivalent to saying that no diffraction patterns will be observed in normal incidence if $\lambda >> \lambda^{*2}$ because $\pi L/2\mu_0$ is generally of the order of unity. At 100 Mcs., λ^{*2} is 225×10^{-8} and λ is already about 25 times and therefore intense diffraction patterns cannot appear in normal

incidence. For higher frequencies, it is still worse and these conclusions are well supported by our observations. It can be easily seen by differentiating (5) that the sharpness of diffraction depends only on the value of $\pi L/\lambda^*$. That is to say, for very high frequencies and large lengths of the sound field, the phenomenon resembles reflection more than diffraction. The sharpness of diffraction does not depend on any other factor like the intensity of the sound field. These conclusions are entirely in conformity with our observations. Using the expression (5), the value of I_{+1}/I_m is calculated for all the four frequencies used and is given in Table IV for a length of sound field of 1 cm. which is the size of the crystal used by us. The intensities are plotted in Fig. 1 keeping I_m constant for all the frequencies. Experimental curves fit extremely well with the theoretical curves. The only point in respect of which there is a discrepancy relates to the gradual fall in intensity as seen in the experimental curves, whereas the theoretical curves show small subsidiary maxima. This is probably due to the fact that the sound field is not the ideal one with undamped amplitude as has been assumed in the theory.

TABLE IV

I_{+1}/I_m	ϕ (177 Mcs)	ϕ102 (Mcs.)	ϕ (50 Mcs.)	ϕ (25 Mcs.)
1	0	0	0	0
·41	1·5′	2·5′	5·1′	10·4′
·09	2·2′	3·8′	7·7′	15·5′
0	2·9′	5·0′	10·3′	20·7′
·045	4·4′	7·5′	15·4′	31′
0	5·8′	10′	20·6′	41·4′
·016	7·3′	12·5′	25·7′	51·3′

It is also seen from equation (5) that the maximum intensity of the first order obtained by tilting the wave front to the appropriate reflection angle is independent of the frequency of the sound wave and is only a function of μ, L and λ.

5. SUMMARY

Diffraction of light by ultrasonic waves of frequencies 25, 50·36, 102·6 and 177·2 Mcs. set up in water has been studied with particular reference to the effect of tilting the wave front. Certain special features which are characteristic of the very high frequencies employed have been observed. The following are the important amongst them. In contrast with the observations at low frequencies, the first order diffraction is predominant at moderately high frequencies like 50 Mcs. and all the higher orders are suppressed. At 100 Mcs. and above, even the first order lines do not appear

for normal incidence but when the sound wave front is tilted from this position to the appropriate side by an angle equal to the Bragg reflection angle, the corresponding order makes its appearance with maximum intensity. At these high frequencies, in no position has it been possible to get both the first order lines on either side of the centre at the same time. For very high frequencies and large lengths of the sound field, the angular range during which a particular diffraction line appears is found to be extremely sharp and narrow. With increasing frequency, the sharpness is found to increase. Experimental observations regarding this sharpness of range are made and compared with the result obtained out of an expression derived from the work of David and Brillouin. The agreement is very satisfactory.

References

1. P. Debye and F. Sears .. *Proc. Nat. Acad. Sci.*, 1932, **18**, 409.
2. R. Lucas and P. Biquard .. *C. R. Acad. Paris*, 1932, **194**, 2132.
3. R. Bär .. *Helv. Phys. Acta.*, 1936, **9**, 265.
4. S. Parthasarathy .. *Proc. Ind. Acad. Sci.*, 1936, **3 A**, 442.
5. ———— .. *Ibid.*, 1936, **3 A**, 594.
6. S. M. Rytov .. *Phys. Zeits. d. Sowjetunion*, 1935, **8**, 626.
7. W. Korff .. *Phys. Zeitschr*, 1936, **37**, 708.
8. C. V. Raman and N. S. Nagendra Nath .. *Proc. Ind. Acad. Sci.*, 1936, **3 A**, 499.
9. N. S. Nagendra Nath .. *Ibid.*, 1937, **4 A**, 222.
10. E. David .. *Phys. Zeit.*, 1937, **38**, 587.

STUDIES IN ATMOSPHERIC OZONE

Part II. Daily Measurements of Atmospheric Ozone and of (δ'-δ''), a Measure of Atmospheric Turbidity, at Delhi

By R. V. Karandikar, M.Sc.

Received June 12, 1948
(Communicatd by Dr. K. R. Ramanathan, M.A., D.Sc., F.A.Sc.)

§1. Introduction

The greater part of our knowledge of atmospheric ozone has come from spectrophotometric measurements of solar radiation in the Hartley absorption band in the near ultra-violet. Starting from the work of Fabry and Buisson,[1] Dobson and co-workers[2] have improved and simplified the methods of observation and made extensive surveys of atmospheric ozone including its general distribution over the earth,[3, 4, 5] the dependence of the total ozone amount on meteorological conditions in Europe,[5, 6, 7] and its distribution in the vertical.[8, 9] Recently, Dr. Dobson[10] with Drs. Brewer and Cwilong has summarised the present position regarding the role of ozone in meteorology.

Measurements of atmospheric ozone in low latitudes are few. For one year in 1929, measurements were made at the Solar Physics Observatory, Kodaikanal[3] with Dobson's photographic photometer, forming part of Dobson's world-wide survey of atmospheric ozone. A further study was made by Dr. Chiplonkar[11] at Bombay during the period 1936–38 using the same photographic instrument. He found general agreement with the Kodaikanal results in respect of seasonal variation, but could find no correlation between the daily values of ozone and surface meteorological conditions.

The most convenient instrument for measuring atmospheric ozone is Dobson's photo-electric spectrophotometer.[12, 13] The photo-electric instrument has great advantages over the photographic one, owing to its greater sensitivity, accuracy and ease of measurement. The instrument is sufficiently sensitive for measurements to be made of the light scattered by the zenith sky even when the sun is slightly below the horizon. This enables the vertical distribution of ozone to be investigated. One of the instruments was acquired in 1940 by the India Meteorological Department. The instrument was set up and preliminary measurements were made by

Dr. Ramanathan and co-workers,* but war-time work prevented the continuation of the work. The present writer began to work with the instrument in 1945.

In view of the fact that during the winter and the following dry season, western disturbances regularly travel across North India, it was considered desirable to take regular observations at Delhi for at least a year. Daily observations were accordingly commenced at Delhi in November 1945 and the results of measurements of the atmospheric ozone during the period November 1945 to March 1947 are discussed in this paper. The effects of dust and haze on ozone measurements came up prominently for attention in the course of the observations at Delhi and this has been discussed in another paper.[14]

§2. Brief Description of the Instrument and the Method of Calculating the Ozone Amount

The instrument consists of a quartz monochromater for isolating the wavelengths 3110 A and 3300 A and a photo-electric cell and amplifier for measuring their relative intensities. The light of the two wavelengths is made to fall on the photo-electric cell one after the other, a rotating shutter admitting one wavelength in two opposite quarters of a rotation and the other wavelength in the other two quarters. By means of a calibrated optical wedge, the light of the wavelength which produces the greater photo-electric current can be cut down so that there are no jumps in current when light of one wavelength is replaced by that of the other. The thickness of the optical wedge in that condition gives a measure of the relative intensities of the two lines. In order to get an estimate of the difference in intensities caused by the difference in scattering at the two wavelengths by air molecules, and by dust, particles of ice or water, measurement is also made of the ratio of intensities of 3300 A and 4450 A (a wavelength well outside the ozone absorption band). By calculation from this, the relative loss of intensity due to scattering at 3300 A and 3110 A is determined and allowed for. The zenith distance of the sun is obtained from the time of observation, using a chart similar to the one described by Dr. Karle Schütte in *Meteorologische Zeitschrift*, 1931. Both the airmass m and the path length μ through the ozone region, each expressed in terms of its normal thickness, are obtained from the zenith distance. For calculating μ, the curves supplied with the instrument, which assumed the mean height of ozone to be 22 km., have been used. According to the later analysis made in another paper,[15]

* Mainly Dr. R. Ananthakrishnan and Mr. S. P. Venkiteshwaran.

it is found that the mean height of ozone over Delhi is 25–27 km. This difference in mean height from the assumed height of 22 km. causes an error in the calculated value of the ozone amount x of about 0·1% at $Z = 50°$, 0·2% at $Z = 60°$, 0·5% at $Z = 70°$ and 1·2% at $Z = 76°$. Only observations with $Z < 70°$ were used in the calculation of daily ozone amounts.

The total amount of ozone x is calculated by the equation,

$$x = \frac{(L_0 - L) - K'(L' - L'_0) - m\{(\beta_1 - \beta'_1) - K'(\beta'_1 - \beta''_1)\}}{\mu\{(\alpha - \alpha') - K'\alpha'\}} \qquad (1)$$

where $L = \log I/I'$, $L_0 = \log I_0/I_0'$, $L' = \log I''/I'$, $L'_0 = \log I_0''/I_0'$, I, I′, I″ being the intensities of the three wavelengths 3110, 3300 and 4450 A received by the instrument and I_0, I_0', I_0'' the corresponding intensities outside the atmosphere; β_1, β_1', β_1'' the coefficients of attenuation due to Rayleigh scattering; α, α', α'' the absorption coefficients per cm. of ozone at N.T.P. for the three wavelengths; $K' = (\delta - \delta')/(\delta' - \delta'')$ where δ, δ', δ'' are the coefficients of attenuation due to non-molecular particle scattering, it being assumed that δ is proportional to λ^{-n} where n has the value 1·3.

The above formula differs from the one used by Dobson in that the allowance for non-molecular scattering has been made somewhat differently. The question has been fully discussed in a separate paper.[14] The change makes very little difference in the calculated ozone amounts on days with clear skies.

In 1941, Dobson[16] suggested the following revised formula for calculating ozone amounts from direct sun observations:

$$x = \frac{(L_0 - L)}{(\alpha - \alpha')\mu} - \frac{(\beta_1 - \beta'_1)m}{(\alpha - \alpha')\mu}. \qquad (2)$$

If m is small, $m/\mu \simeq 1$ and the value of the second term on the right hand side of the equation according to the values of the constants given by Dobson is 0·085 and is assumed to hold on clear days. The value is increased to 0·095 on hazy days and even to 0·105 on very hazy days. Tonsberg and Olsen[17] in their work at Tromsø, used the following single formula as suggested by Dobson.[16]

$$x = (L_0 - L)/1{\cdot}17\,\mu - 0{\cdot}085 \qquad (3)$$

For comparison, the values calculated according to equations (1), (2) and (3) are given in different columns under x, $x_{D'}$ and x_D respectively in the Appendix. For x and $x_{D'}$, the values of the constants assumed for Delhi and given in the Appendix were used, and the deviation of m/μ from unity at different zenith distances of the sun was also taken into account. For

x_D, equation (3) was used as it is. On clear days, the two formulæ for x and $x_{D'}$ give practically the same values, but on hazy days there are significant differences of opposite signs in the winter and hot seasons respectively. x_D is generally higher than $x_{D'}$ by 0·003 cm.

§3. Recalibration of the Optical Wedges

When work with the instrument was resumed in 1945 at Delhi, the first step taken was to redetermine the values of the constants L_0 and L_0' by extrapolating from the observed values of L and L′ on clear days against the ozone paths at different zenith distances of the sun. The values of L and L′ and of μ were obtained from charts supplied with the instrument. It was found that even on very clear days such plots showed some systematic deviations from the expected straight lines. For calibrating the instrument, the method suggested by Dr. Dobson[18] was employed. The instrument was set so as to pass light of wavelength 3300 A into the photoelectric cell. In that condition, the deflection of the galvanometer was a measure of the intensity of light of this wavelength falling on the photo cell. The wedge was set at some known reading near its thin end and the sensitivity of the instrument adjusted so as to give a convenient deflection in the galvanometer. A thin metal gauze of known transmission ratio was then placed in the path of the beam of light causing a decrease in the deflection of the galvanometer. The gauze was now removed and the same decrease of deflection produced by moving the wedge. The difference between the two wedge readings corresponds to the attenuation caused by the perforated metal gauze.

Some details regarding the calibration may be recorded. The mercury ultra-violet lamp supplied with the instrument was not found to give sufficient light to enable satisfactory readings to be taken in the thicker parts of the wedge. Sunlight on very clear days of settled weather between 10 hours and 14 hours was therefore used for the calibration. A machine-perforated zinc gauze of suitable mesh, blackened chemically with silver nitrate, was used to attenuate the incident sunlight. This was placed immediately in front of the prism of the sun-director and kept moving in its own plane so as to average out non-uniformities due to the finite number and spacing of the holes. Steady deflections were obtained and individual readings could be repeated to within 1°. The mean differences ΔD between the dial readings, with and without the gauze, were determined throughout the range and these were plotted against the mean dial readings (Fig. 1). On the same diagram is also shown the curve that would have been obtained if the calibration chart supplied with the instrument were correct. The observations

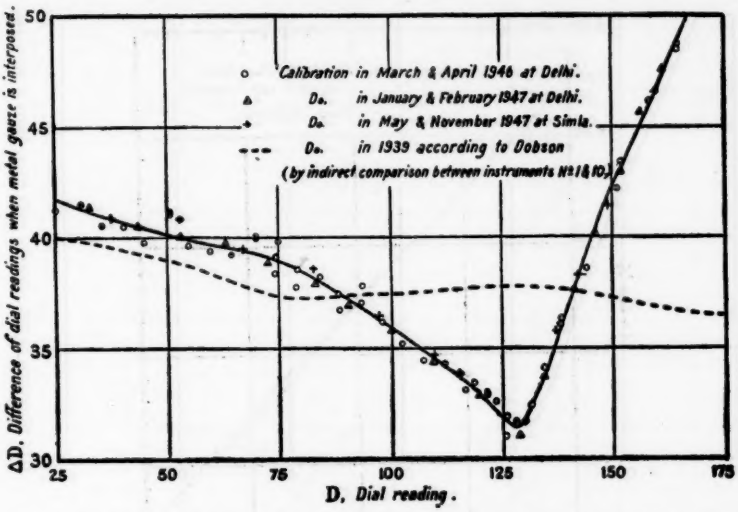

FIG. 1. Calibration of optical wedges in Dobson's ozone spectrophotometer (No. 10) using perforated zinc gauze

were repeated on many clear days in the months of March and April 1946, with different dial readings as starting points. Similar detailed calibration was again done in January and February 1947 at Delhi and in May and November 1947 at Simla. The results are all plotted on the same diagram and show the constancy of the new calibration. Considering that the instrument had been in Delhi throughout the hot summer with temperatures as high as 115° F·, this is a satisfactory result. The mean transmission ratio of the gauze was determined to be 41·05%, the corresponding value of ΔL being 0·387.

From the smooth curve of Fig. 1, $\Delta L/\Delta D$ was calculated for each degree of the dial and with the addition of a suitable constant, the calibration curve of L against D was obtained by taking successive differences. Fig. 2 shows both the old and new calibration curves, the two being made to coincide at 90°. There is increasing deviation between the two curves on either side of 90°, but on the thicker side of the wedges, the curves close up again after 140°. Tables giving log I/I′ for every 0°·1 of the dial were prepared for routine use.

For a number of clear days on which a large number of observations for all heights of the sun were available, L and L′ were plotted against μ. The new chart gave a definitely better straight-line fit of the observations.

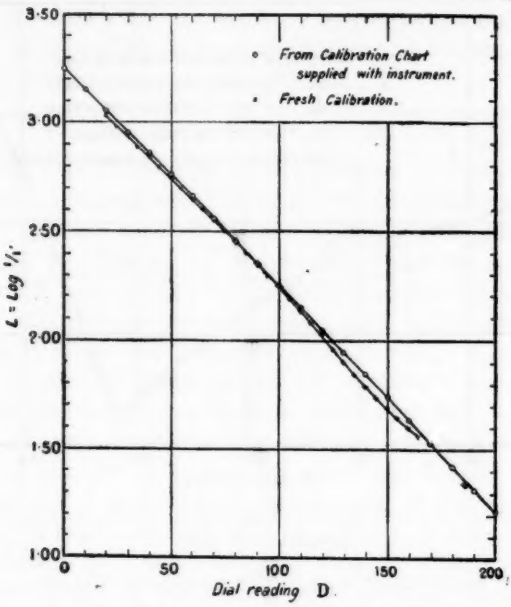

FIG. 2. Old and new calibration curves of optical wedges

As an example, in Fig. 3, the observations on 18–4–1946 are compared with the two calibrations. There is, however, a tendency for the values of L at high values of μ to lie out. This is to be attributed to the incorrectness of the assumption that 22 km. is the mean height of the ozone layer. According to the analysis made in another paper[15] the mean height in India is 25–27 km.

It is now understood from Dr. Dobson[18] that " when the whole batch of new ozone instruments was calibrated, the wedge in the original instrument (No. 1) only was calibrated directly by the detailed method described above; each of the new instruments was calibrated only by comparing with instrument No. 1, simultaneous observations being taken at all heights of the sun with the two instruments. This method was quicker and it was expected that the results of all instruments would be exactly comparable ". In view of the experience with instrument No. 10, it seems desirable to calibrate each instrument individually with a sufficiently intense source of ultraviolet radiation. In India, with the high noon-day sun, advantage can be taken of clear days for the calibration.

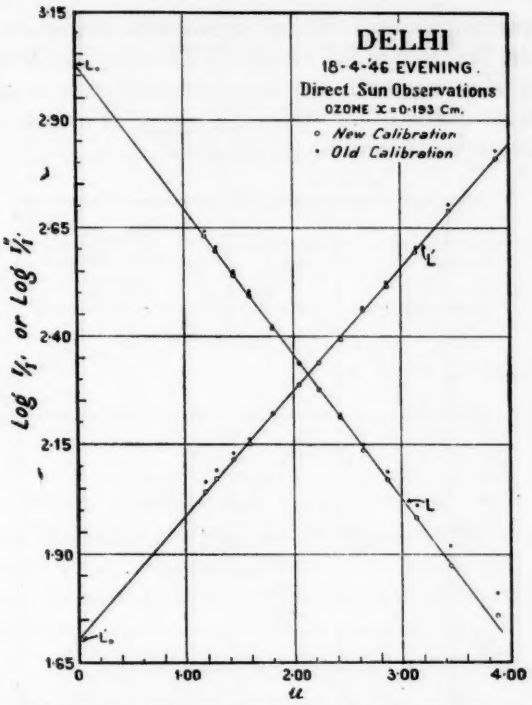

FIG. 3. Use of old and new calibration curves to determine the constants L_0 and L_0'

§4. DETERMINATION OF THE CONSTANTS L_0 AND L_0' FOR THE INSTRUMENT

L_0 and L_0' correspond to the ratios of the intensities of 3110 A and 3300 A, and of 4450 A and 3300 A outside the atmosphere. To obtain these, the values of L and L′ obtained on a number of clear days with all heights of the sun were plotted against corresponding values of μ, and the values for $\mu = 0$ were obtained by extrapolation. The values of μ for different zenith-distances were taken from the chart supplied with the instrument, and this corresponds to 22 km. for the mean height of the ozone layer. Even if the mean ozone height over Delhi differs somewhat from 22 km., no appreciable error in the determination of L_0 and L_0' will be caused if values of μ greater than 3·5 or 4 are not taken into consideration for the extrapolation. The mean of 60 such determinations on clear days gave $L_0 = 3{\cdot}020$ and $L_0' = 1{\cdot}715$, the extreme values of L_0 being 3·004 and 3·033 and those of L_0' 1·700 and 1·733. Individual days' values show a random scatter and o regular drift.

It is interesting to note that no appreciable changes in the values of L_0 and L'_0 were observed in the months of February and March 1946, when large sunspots were reported. On the other hand, haze caused appreciable disturbance in the course of the values of L and L′ as will be seen from Fig. 4 which relates to a very hazy day (17–11–1945).

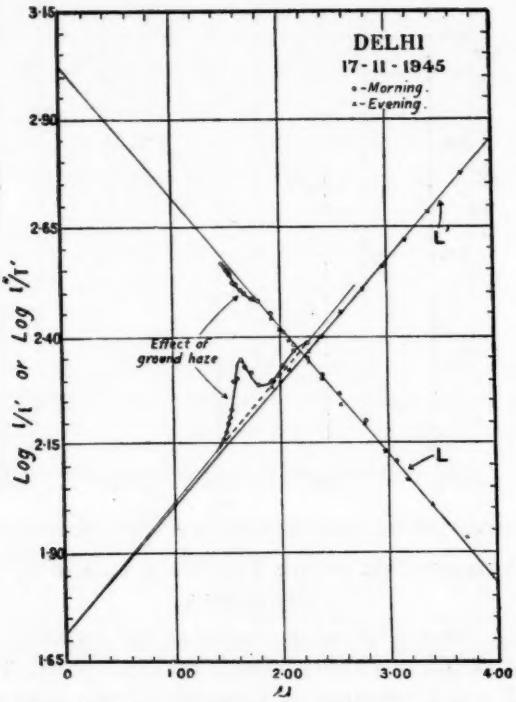

FIG. 4. Direct sun observations on a very hazy day

§5. DIURNAL VARIATION OF ATMOSPHERIC OZONE

Observations with direct sunlight made at different times of the day show a small systematic daily variation of ozone amount. Fig. 5 *a* shows the variation on six consecutive clear days in September 1946; Fig. 5 *b* shows similar curves for a few days in other months. The afternoon values in all instances are higher than the morning ones; there is also a marked dip at about local noon. This dip at noon is not of instrumental origin since the calibration of the wedges had been carefully checked and also the observations with high sun could be obtained without ambiguity.

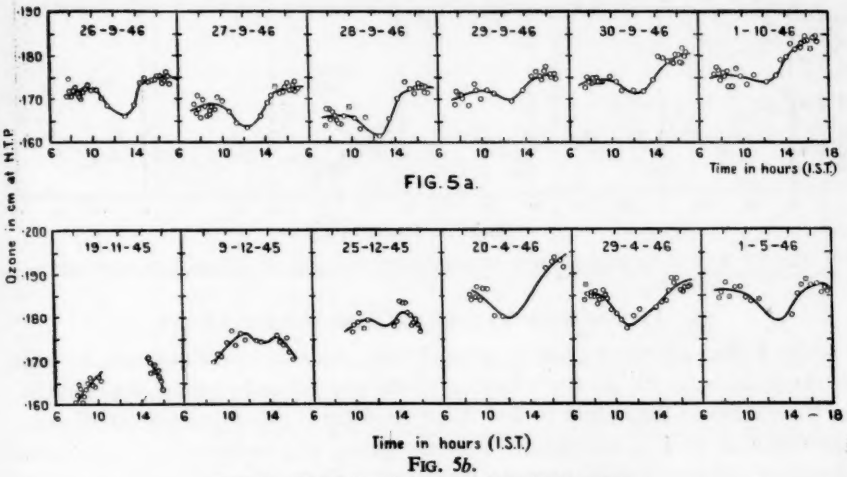

FIG. 5. Diurnal variation of atmospheric ozone

Fig. 6 shows the mean morning and afternoon values of ozone for a number of days on which observations were taken both in the morning and in the afternoon. In almost all cases, the afternoon values were higher than the morning ones.

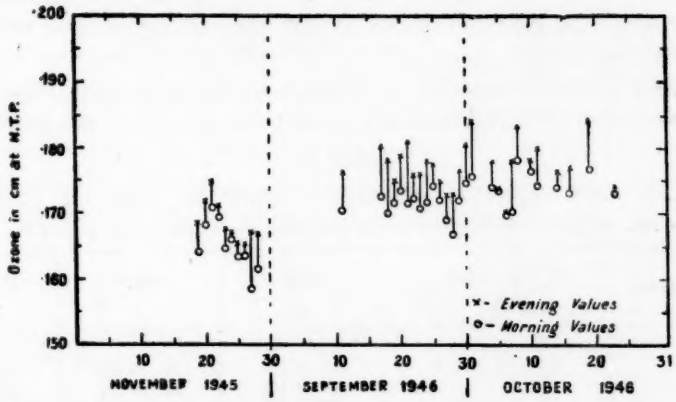

FIG. 6. Morning and evening values of atmospheric ozone on a number of days

There are, however, instances when the morning values were higher than the afternoon ones. Such days were rare and generally occurred when the daily ozone amounts were falling. Fig. 7 gives the results for a few such consecutive days.

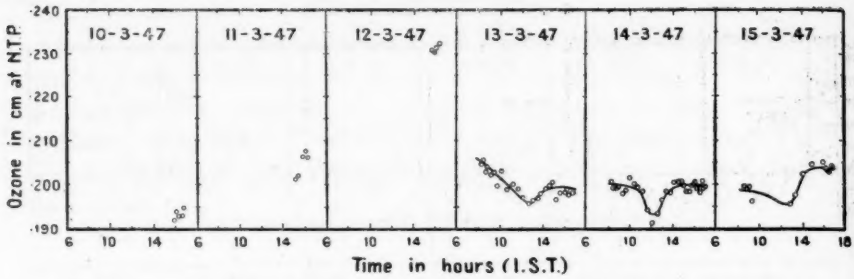

FIG. 7. Diurnal variation of ozone on consecutive days when the values of the ozone amount are falling

§6. DAY-TO-DAY VALUES OF ATMOSPHERIC OZONE

In India, whenever there is ground haze, even of small amount, it rises in the forenoon with the sun's heating of the ground and causes a disturbance in the course of the values of L. After the haze is dissipated by turbulence, the variation of L is smoother. For comparing day-to-day values of ozone, therefore, afternoon measurements were used. Only when afternoon observations could not be had for any reason, were morning observations used for the comparison.

Fig. 8 shows the daily mean afternoon values of the total amount of atmospheric ozone at Delhi during the period November 1945 to March 1947. These are on the basis of direct sun observations and generally refer to afternoon. The gaps correspond to days when cloudy weather prevented direct sun observations.

Table I gives the monthly mean values of ozone at Delhi during the period November 1945 to March 1947, and these are also shown graphically

TABLE I

Monthly mean values of atmospheric ozone at Delhi (28° 35′ N.)

n = No. of days of observations (direct sun only), x = Ozone in cm. at N.T.P.

Month	1945		1946		1947		Mean
	n	x	n	x	n	x	x
January ..			28	0·170	18	0·192	0·181
February ..			22	0·173	26	0·197	0·185
March ..			28	0·183	24	0·198	0·191
April ..			30	0·188			0·188
May ..			29	0·187			0·187
June ..			28	0·189			0·189
July ..			21	0·179			0·179
August ..			21	0·173			0·173
September ..			28	0·176			0·176
October ..			21	0·179			0·179
November ..	19	0·169	29	0·175			0·172
December ..	27	0·170	28	0·182			0·176

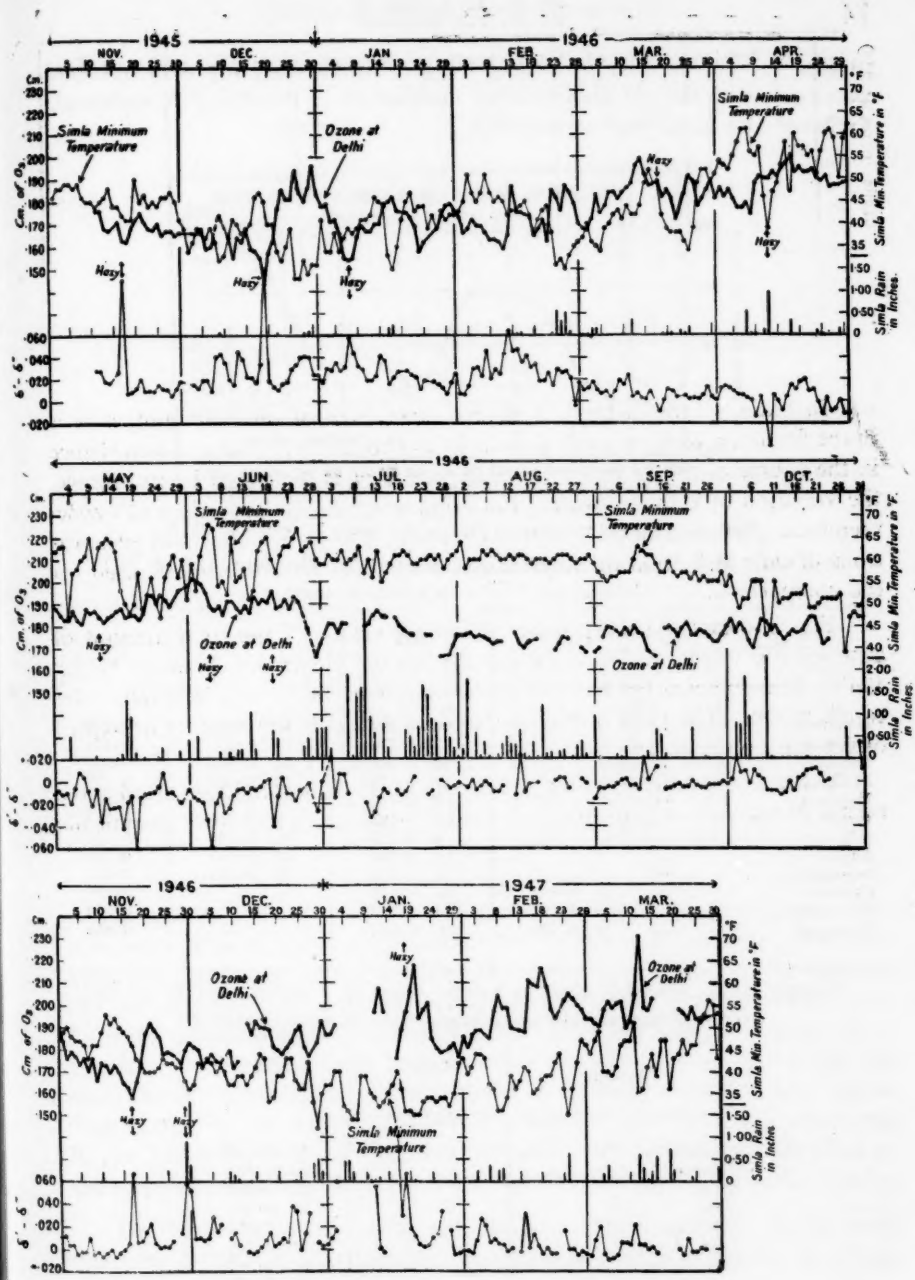

FIG. 8. Daily values of afternoon ozone amounts and atmospheric turbidity ($\delta' - \delta''$) at Delhi and of minimum temperatures and rainfall recorded at 0800 hrs. at Simla, during November 1945 to March 1947.

in Fig. 9. Tables 2 to 5 and Fig. 10 give similar monthly data obtained previously with the old photographic instruments at Bombay,[11] Kodaikanal,[3] Helwan[3] and Zi-ka-wei[4] respectively.

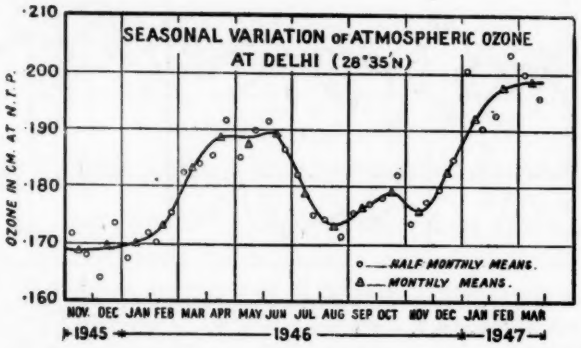

FIG. 9. Seasonal variation of atmospheric ozone at Delhi (28° 35′ N.)

TABLE II. *Monthly mean values of ozone at Bombay* (18° 54′ N.)
(From Dr. Chiplonkar's measurements)

Month	1936		1937		1938		Mean
	n	*x*	*n*	*x*	*n*	*x*	*x*
January ..			26	0·215	30	0·205	0·210
February ..			17	0·234	28	0·213	0·221
March ..			29	0·210	31	0·215	0·213
April ..			28	0·219	27	0·229	0·224
May ..			3	0·191	28	0·224	0·221
June ..			2	0·188	9	0·220	0·214
July ..			4	0·179	11	0·223	0·211
August ..			14	0·194	10	0·207	0·199
September ..			15	0·214	16	0·213	0·213
October ..	10	0·217	28	0·219			0·218
November ..	2	0·196	22	0·205			0·204
December ..	9	0·213	31	0·207			0·208

TABLE III. *Monthly mean values of ozone at Kodaikanal* (10° 10′ N.)
(From Dobson and Harrison's measurements of Kodaikanal plates)

Month	1928		1929	
	n	*x*	*n*	*x*
January ..			24	0·192
February ..			24	0·194
March ..			23	0·199
April ..			15	0·204
May ..			18	0·211
June ..			7	0·209
July ..			14	0·211
August ..			19	0·205
September ..	17	0·206		
October ..	12	0·2025		
November ..	7	0·193		
December ..	12	0·189		

TABLE IV. *Monthly mean values of ozone at Helwan (Egypt, 29° 50° N.)*

Month	1928		1929	
	n	*x*	*n*	*x*
January ..			23	0·233
February ..			18	0·237
March ..			15	0·250
April ..			17	0·246
May ..			..	..
June ..			..	..
July ..			8	(0·230)
August ..			20	0·231
September ..			23	0·232
October ..	9	(0·214)	6	(0·215)
November ..	16	0·207		
December ..	22	0·211		

TABLE V. *Monthly mean values of ozone at Zi-ka-wei (Shanghai, 31° N.)*

(From Rev. P. Lejay's measurements)

Month	1932	1933	1934	1935	1936	Mean
January ..	0·212	0·254	0·248	0·255	0·267	0·247
February ..	0·243	0·263	0·251	0·279	0·275	0·262
March ..	0·262	0·262	0·268	0·266	0·275	0·267
April ..	0·249	0·254	0·251	0·259	0·281	0·259
May ..	0·241	0·255	0·250	0·263	0·269	0·256
June ..	0·240	0·258	0·242	0·248	0·210	0·240
July ..	0·226	0·232	0·230	0·227	0·229	0·229
August ..	0·229	0·239	0·226	0·224	0·240	0·232
September ..	0·233	0·231	0·222	0·230	0·231	0·229
October ..	0·226	0·211	0·220	0·222	0·225	0·221
November ..	0·221	0·206	0·204	0·211	0·214	0·211
December ..	0·219	0·231	0·221	0·225	0·221	0·223

In general, the maximum ozone values occur in April-June. The minimum seems to occur in November but there is a pronounced secondary minimum in the monsoon months July-August. Curves for Kodaikanal and Bombay and also those for Helwan and Zi-ka-wei show similar features. Even for the same place, the monthly means for two successive years differ appreciably as is seen from both Bombay and Delhi data. At Delhi, for example, the ozone values for the winter of 1946–47 were definitely higher than those for the winter of 1945–46. Similar differences are observable in the Tromsø[16] data for the years 1939–42. Any definite latitude effect in the tropics cannot be established from the observations so far made in India.

On the average, the ozone amount over Delhi appears smaller than that over Bombay or Kodaikanal. It should be remembered that the photo-

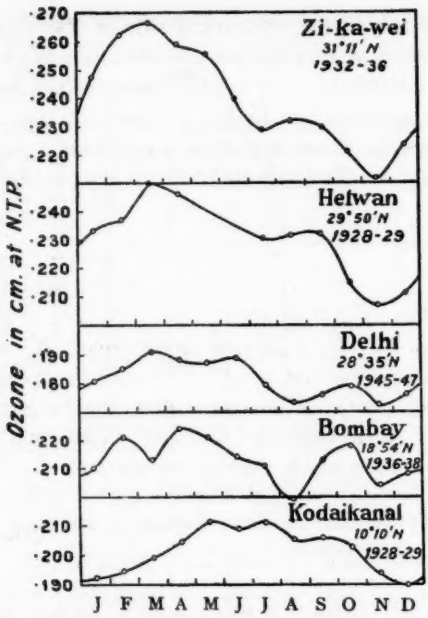

FIG. 10. Annual variation of atmospheric ozone in low latitudes

graphic instrument was used at the latter two places and that a modified formula with slightly different constants was used for calculating the ozone amounts over Delhi.

§7. DAILY VALUES OF $(\delta'-\delta'')$, A MEASURE OF ATMOSPHERIC TURBIDITY

In obtaining the final equation 2 (1) for x, it was assumed that for the pair of longer wavelengths,

$$\log I''/I' = \log I_0''/I_0' + \alpha' x\mu + (\beta_1' - \beta_1'')\, m + (\delta' - \delta'')\, m \qquad (4)$$

where the symbols have the meaning stated in §2.

This leads to

$$(\delta' - \delta'')\, m = (L' - L_0') - \alpha' x\mu - (\beta_1' - \beta_1'')\, m \qquad (5)$$

i.e.,
$$(\delta' - \delta'') = (L' - L_0')/m - \alpha' x.\ \mu/m - (\beta_1' - \beta_1'') \qquad (6)$$

If observations are taken for small values of m, the ratio μ/m is very nearly equal to unity and we get

$$\delta' - \delta'' \fallingdotseq (L' - L_0')/m - \alpha' x - (\beta_1' - \beta_1'') \qquad (7)$$

Here the first term on the right-hand side of the equation corresponds to the incident radiation, the second term to the attenuation due to absorption by ozone, and the last to the attenuation due to molecular scattering. The left-hand side thus corresponds to the fraction of the incident radiation scattered by the large particles, and thus may be taken as a measure of the atmospheric turbidity in the long-wavelength region (3300 to 4450 A).

The above expression for $(\delta' - \delta'')$ can be easily calculated directly from the observations for the pair of longer wavelengths, if the value of x is roughly known and the value of $(\beta_1' - \beta_1'')$ for molecular scattering is assumed for the place of observation. Normally δ' is greater than δ'' and hence the expression $(\delta' - \delta'')$ should be positive. If, however, $(\delta' - \delta'')$ is found to be negative, it would mean either that (*a*) the attenuation due to particle scattering at 3300 A is *less than* that due to particle scattering at 4450 A, which is rather anomalous, or that (*b*) the instrument is analysing not directly transmitted sunlight alone, but an additional radiation richer in shorter wavelengths goes into the instrument. A value of $\delta' - \delta''$ nearly equal to zero would mean that the scattering corresponds to sufficiently large particles so as to make it practically neutral.

Daily values of $\delta' - \delta''$ were calculated along with the ozone values for the period November 1945 to March 1947 and these are tabulated in the Appendix, together with the remarks about the sky condition on each day. These are also plotted along with the ozone values in Fig. 8.

An inspection of the plot suggests the following general conclusions:—

(*a*) On average clear days, $\delta' - \delta''$ is positive during the period November to March, mostly negative during the period April to July, and near about zero during the rest of the year.

(*b*) On hazy days, the numerical value of $\delta' - \delta''$ increases with increase in haziness in all the seasons.

In a previous paper,[14] an explanation is given of the unexpected new feature about the negative sign of $\delta' - \delta''$ (*i.e.*, apparently greater loss due to scattering at 4450 A than at 3300 A) in the pre-monsoon period, particularly on days when there was widespread milky haze over the sky. A suitable modification in the formula for the calculation of the value of total ozone x was also suggested. Here, the values of $\delta' - \delta''$ are simply tabulated as a convenient measure of the atmospheric turbidity and may be compared with the remarks by visual observation about the sky condition.

§8. Correlation with Meteorological factors

The daily ozone values at Delhi were plotted side by side with various meteorological factors, such as the pressure at 0800 hrs. at Delhi and Simla, rainfall, minimum temperature, etc. Out of these, Simla minimum temperature showed a significant negative correlation with daily ozone values at Delhi during some non-monsoon months when western disturbances passed regularly. The minimum temperatures at Simla were, however, frequently affected by rainfall or föhn action. This is clearly seen in Fig. 8, which gives daily ozone values at Delhi along with minimum temperatures and daily rainfalls at Simla. Although higher correlation was expected with upper air data, comparison with available upper winds and radiosonde temperatures at 6 km. over Delhi did not show any definite correlation.

Table VI gives the standard deviations and correlation coefficients between Delhi ozone amounts and Simla minimum temperatures both month

Table VI. *Correlation between Delhi ozone amounts (x) and Simla minimum temperatures (y)*

N= number of observations in the period

Month	N	Standard Deviation		Correlation Coefficient r	$Z = \frac{1}{2}\log_e\frac{1+r}{1-r}$	Standard error $\pm 1/\sqrt{N-3}$
		Ozone $\sigma x\ 10^{-3}$ cm.	Min. Temp. σy °F.			
November 1945 ..	19	3·9	2·3	+0·26	+0·27	±0·250
December 1945 ..	29	12·7	5·0	−0·86	−1·29	±0·196
January 1946 ..	29	7·7	4·3	−0·11	−0·11	±0·196
February 1946 ..	28	7·8	5·6	−0·63	−0·74	±0·200
March 1946 ..	29	7·4	5·7	+0·22	+0·23	±0·196
November 1945 to March 1946 ..	134	10·2	5·5	−0·20	−0·20	±0·087
April 1946 ..	30	6·2	5·3	−0·28	−0·29	±0·193
May 1946 ..	29	4·4	5·8	−0·36	−0·38	±0·196
June 1946 ..	28	7·2	4·9	+0·02	+0·02	±0·200
July 1946 ..	21	5·4	2·0	−0·31	−0·32	±0·236
August 1946 ..	21	2·8	0·9	−0·05	−0·05	±0·236
September 1946 ..	28	3·5	2·1	−0·17	−0·17	±0·200
October 1946 ..	25	4·6	3·2	−0·33	−0·34	±0·213
April 1946 to October 1946 ..	182	7·9	5·1	−0·13	−0·14	±0·075
November 1946 ..	29	7·9	4·4	−0·49	−0·54	±0·196
December 1946 ..	28	6·5	3·7	−0·19	−0·19	±0·200
January 1947 ..	20	10·9	3·8	−0·58	−0·66	±0·243
February 1947 ..	26	9·1	4·4	−0·40	−0·43	±0·209
March 1947 ..	24	7·9	4·5	−0·50	−0·55	±0·218
November 1946 to March 1947 ..	127	12·4	5·6	−0·37	−0·39	±0·090

by month and collectively for the three periods November 1945 to March 1946, April 1946 to October 1946 and November 1946 to March 1947. In December 1945 and February 1946, the correlations were high and negative (− 0·86 and − 0·63 respectively). In other months the correlations were less marked, and there are also three months with positive correlation. The last two columns give an idea of the significance of these correlations on applying the Z significance test.

The day-to-day changes in ozone amount were conspicuous during the period of western disturbances. In general, northerly air was found to be associated with high ozone amounts. Any association of changes of ozone amount with fronts has not yet been established. In the monsoon season, the average ozone amount was low and the day-to-day fluctuations were also small. The stabilizing effect of the monsoon on the total ozone amount in the atmosphere at a low value suggests that water vapour in the upper troposphere has a destructive action on ozone. During the monsoon, the tropopause in North India is almost always of Type I, beginning with a strong inversion at a height of 16–17 km. Mixing from below up to the tropopause would then be a normal feature.

§9. Effect of Thunderstorms

Direct sun observations before and after thunderstorms were made on a few occasions (11–4–46, 22–4–46, 30–4–46, 4–5–46, 20–5–46, 6–6–46, 15–8–46); observations were also made during thunderstorms with light rain falling from thundering cumulonimbus clouds overhead. In no case was any significant change in the ozone content observed. Later at Simla also, on 5–5–47, direct sun observations were made with thunder clouds all around and heavy hailstorms before and after observations; but no significant rise in ozone content was observed. The above result is at variance with Dobson's recent finding[10] that a sudden rise in ozone, within a short period of one or two hours, from 0·250 to 0·475 cm. occurred during a thunderstorm on 13th July 1941. He attributes this high rise in ozone to electrical disturbances during thunderstorms and states that 'most of the ozone formed during thunderstorms is almost certainly situated within the thunder cloud and not in the stratosphere. Such observations have necessarily to be made on the cloudy sky and are much less accurate than observations with sunlight. It is probable, however, that any error involved will make the observed value too small rather than too great'. Dobson's results were based on observations on cloudy zenith sky, but one would have expected similar changes to be observable with direct sun observations also in the neighbourhood of thundering clouds. The discrepancy remains to be explained.

There was only one occasion (13th March 1947) when an appreciable rise in ozone amount was noticed (from 0·190 to 0·230 cm.). But this thunderstorm occurred late in the evening, three to four hours after the high value of ozone was observed by means of direct sunlight observations. On that day, there was a depression over Rajputana, roughly 300 miles southwest of Delhi. Apparently, changes in ozone content associated with some western disturbances do occur, but changes directly connected with individual thunderclouds have been difficult to find.

§10. Effect of Magnetic Disturbances and Sun-spots

No quantitative correlation could be established between the daily magnetic character figures from records at Alibag and the daily ozone amounts. There were also no marked changes in ozone when big sun-spots and associated solar disturbances were reported in the months of February and March 1946.

§11. Concluding Remarks

The marked correlation of ozone amounts with Simla minimum temperatures suggests that changes of air-mass at high levels containing appreciable quantities of ozone do occur in the season of western disturbances, northerly air from higher latitudes bringing with it more ozone. The day-to-day changes in ozone amounts are much less pronounced than in temperate latitudes. For an adequate study of the distribution of ozone in the field of cyclones and anti-cyclones, simultaneous observations at a few more stations are necessary. During the monsoon months, the ozone amount is insensitive to surface conditions, suggesting that tropical ozone exists mostly high up in the atmosphere in a region little disturbed by surface weather changes.

§12. Acknowledgments

The observations were made with the Dobson spectrophotometer belonging to the India Meteorological Department and the author's thanks are due to the Director-General of Observatories for the use of the instrument and for giving all necessary facilities. The author wishes to express his grateful thanks to Prof. K. R. Ramanathan, who initiated the present scheme and under whose direction the work was carried out. Thanks are also due to the Board of Scientific and Industrial Research for the award of a Research Fellowship during the period in which the work was done.

Summary

Daily measurements of the total amount of atmospheric ozone were made at Delhi with Dobson's photo-electric ozone spectrophotometer during

the period November 1945 to March 1947. The optical wedges in the instrument required a recalibration and this was done carefully by a detailed method using perforated metal gauzes of known extinction. The constancy of the calibration was checked on a number of occasions during the period of observations. The constants L_0 and L_0' of the instrument were determined from the plots of the observations on a number of selected clear days.

An attempt to study the diurnal variation of ozone on many clear days showed that the afternoon values were generally higher than the morning ones with a marked dip at about the local noon. But there were some days with practically constant ozone and very occasionally, days with afternoon values lower than the morning ones.

The daily afternoon values of ozone from direct sun observations were plotted throughout the period of observation along with a number of meteorological factors. Simla minimum temperatures showed a significant negative correlation with ozone amounts, particularly during the non-monsoon seasons when western disturbances were prevalent. The significance of this is discussed. The minimum temperatures on some days were considerably affected by rainfall or by föhn-effect. There is no evident relation between the daily ozone variations and the magnetic character figures or sun-spots. Duststorms, thunderstorms and cumulonimbus clouds did not show any significant changes in ozone. This result differs from Dobson's recent findings and requires further investigation.

As regards annual variations, the maximum ozone values occur in April-May and the minimum in November with another pronounced secondary minimum in August. This was in agreement with previous observations at Kodaikanal and Bombay and at Helwan and Zi-ka-wei. The ozone values in November 1946 to March 1947 were markedly larger than those in November 1945 to March 1946.

Daily values of $(\delta' - \delta'')$, where δ', δ'' are the net losses due to particle scattering at the wavelengths 3300 and 4450 A respectively, are tabulated. This can be taken as a convenient measure of the atmospheric turbidity in this wavelength region. An unexpected new feature is the negative sign of $\delta' - \delta''$ (that is, apparent greater loss due to scattering at 4450 A than at 3300 A) in the pre-monsoon period, particularly on days when there is a widespread milky haze over the sky.

On the whole, the results show that the day-to-day variations in ozone amounts are small during the monsoon, but quite conspicuous during the

season of western disturbances. In general, northerly air is found to be associated with high ozone amounts.

References

1. C. Fabry and H. Buisson .. *J. Physique*, 1913, **3**, 196.
   ———— .. *Astrophys. Journ.*, 1921, **54**, 297.
2. (*a*) G. M. B. Dobson and D. N. Harrison .. *Proc. Roy. Soc.*, A, 1926, **110**, 660.
   (*b*) G. M. B. Dobson, D. N. Harrison and J. Lawrence .. *Ibid.*, 1927, **114**, 521.
   (*c*) ———— .. *Ibid.*, 1929, **122**, 456.
3. ———— .. *Ibid.*, 1930, **129**, 411.
4. Rev. P. Lejay .. *Notes de Météorologie Physique*, 1937, Fascicule VII.
5. G. M. B. Dobson and A. R. Meetham .. *Quar. Jour. Roy. Met. Soc.*, 1934, **60**, 265.
6. G. M. B. Dobson .. *Ibid.*, 1936, Suppl. to Vol. **62**, 52.
7. (*a*) A. R. Meetham .. *Ibid.*, 1936, Suppl. to Vol. **62**, 59.
   (*b*) ———— .. *Ibid.*, 1937, **63**, 289.
8. F. W. P. Götz, A. R. Meetham and G. M. B. Dobson .. *Proc. Roy. Soc.*, A, 1934, **145**, 416.
9. A. R. Meetham and G. M. B. Dobson.. *Ibid.*, 1935, **148**, 598.
10. G. M. B. Dobson, Brewer and Cwilong .. "Bakerian Lecture," *Ibid.*, 1946, **185**, 144.
11. M. W. Chiplonkar .. *Proc. Ind. Acad. Sci.*, A, 1939, **10**, 105.
12. G. M. B. Dobson .. *Proc. Phys. Soc.*, 1931, **43** III, 324.
13. ———— .. "Instructions for use of Dr. Dobson's spectrophotometer," R. and J. Beck Ltd., London.
14. K. R. Ramanathan and R. V. Karandikar .. "Effect of dust and haze on measurements of atmospheric ozone made with Dobson's ozone spectrophotometer." In course of publication.
15. R. V. Karandikar and K. R. Ramanathan .. "Vertical distribution of ozone over Delhi." In course of publication.
16. "Dobson's circular to workers on ozone," 1941.
17. E. Tonsberg and K. L. Olsen .. "*Geophys. Publikas., Utgitt. av det Norske Videnskaps–Akademi*, Oslo, Vol. XIII, No. 12, 1944.
18. Dobson's note on the calibration of the optical wedges in the ozone spectropotometer.—5-4-44.

APPENDIX

Daily values of atmospheric ozone and of $(\delta' - \delta'')$, *a measure of atmospheric turbidity, at Delhi for four specimen months during the period November* 1945 *to March* 1947

SYMBOLS

x = ozone in cm. at N.T.P. according to the newly proposed equation (1),

$$= \frac{(L_0 - L) - K'(L' - L_0') - m\{(\beta_1 - \beta_1') - K'(\beta_1' - \beta_1'')\}}{\mu\{(\alpha - \alpha') - K'\alpha'\}}$$

where $K' = 0{\cdot}249$, $\alpha = 1{\cdot}275$, $\alpha' = 0{\cdot}074$,

$\beta_1 - \beta_1' = 0{\cdot}0965$, $\beta_1' - \beta_1'' = 0{\cdot}2515$,

$(\beta_1 - \beta_1')/(\alpha - \alpha') = 0{\cdot}080$;

$x_{D'}$ = ozone in cm. at N.T.P. according to Dobson's revised formula (2) and with the values of the constants used as given above,

$$= \frac{L_0 - L}{\mu(\alpha - \alpha')} - \frac{\beta_1 - \beta_1'}{\alpha - \alpha'} \cdot \frac{m}{\mu} = \frac{L_0 - L}{1{\cdot}201\,\mu} - 0{\cdot}080\, m/\mu\ ;$$

x_D = ozone in cm. at N.T.P. according to Dobson's formula (3) and with the same values of constants as used by Dobson.

$$= \frac{L_0 - L}{1{\cdot}17\mu} - \frac{0{\cdot}10}{1{\cdot}17} = \frac{L_0 - L}{1{\cdot}17\,\mu} - 0{\cdot}085\ ;$$

δ' = scattering coefficient for large particles at 3300 A for the whole of the atmosphere over Delhi.

δ'' = the same at 4450 A.

ABBREVIATIONS

b = clear blue sky, B = deep blue sky;

z_0 = slightly hazy, z = hazy, Z = very hazy;

c_0 = slightly cloudy, c = cloudy, o = overcast.

Date	December 1945					March 1946				
	Sky	$\delta'-\delta''$	x	$x_{D\theta}$	x_D	Sky	$\delta'-\delta''$	x	$x_{D\theta}$	x_D
1	o ..	..	..	..	..	b ..	0·010	0·168	0·170	0·173
2	o ..	..	..	..	..	c ..	0·013	0·167	0·170	0·173
3	b ..	0·015	0·166	0·169	0·173	c ..	0·017	0·171	0·174	0·177
4	b ..	0·012	0·166	0·169	0·172	c_0 ..	0·011	0·183	0·185	0·188
5	c_0 ..	0·019	0·168	0·172	0·175	c_0 ..	0·007	0·175	0·177	0·180
6	b ..	0·019	0·159	0·163	0·167	c_0 ..	0·009	0·178	0·180	0·183
7	c_0 ..	0·009	0·160	0·162	0·165	c_0 ..	0·004	0·184	0·185	0·188
8	z_0 ..	0·040	0·163	0·171	0·174	c ..	0·009	0·184	0·186	0·189
9	z_0 ..	0·043	0·174	0·183	0·186	c ..	0·019	0·181	0·185	0·188
10	b ..	0·035	0·175	0·183	0·185	b ..	0·015	0·184	0·187	0·190
11	b ..	0·019	0·164	0·169	0·171	b ..	0·024	0·186	0·191	0·195
12	b ..	0·015	0·155	0·159	0·162	b ..	0·004	0·188	0·189	0·193
13	B ..	0·045	0·164	0·173	0·176	B ..	0·007	0·195	0·197	0·200
14	b ..	0·038	0·162	0·170	0·173	c_0 ..	0·003	0·199	0·199	0·203
15	b ..	0·022	0·167	0·171	0·174	b ..	0·002	0·192	0·193	0·196
16	B ..	0·021	0·159	0·164	0·166	c ..	0·009	0·187	0·189	0·192
17	c_0 ..	0·017	0·158	0·161	0·164	o ..	..	..	..	..
18	c_0 ..	0·033	0·155	0·162	0·164	z ..	−0·009	0·189	0·187	0·190
19	Z ..	0·120	0·143	0·169	0·171	b ..	0·001	0·182	0·183	0·186
20	b ..	0·019	0·157	0·161	0·164	b ..	0·011	0·185	0·187	0·191
21	b ..	0·013	0·161	0·164	0·167	b ..	0·009	0·181	0·183	0·186
22	b ..	0·010	0·177	0·179	0·182	z_0 ..	0·004	0·172	0·173	0·176
23	b ..	0·017	0·185	0·188	0·191	o ..	..	..	..	..
24	b ..	0·018	0·181	0·185	0·188	b ..	0·005	0·183	0·185	0·188
25	b ..	0·029	0·182	0·188	0·191	B ..	0·002	0·191	0·191	0·194
26	z_0 ..	0·033	0·194	0·201	0·205	b ..	0·003	0·189	0·190	0·193
27	z_0 ..	0·041	0·184	0·193	0·197	b ..	0·003	0·178	0·179	0·182
28	b ..	0·041	0·180	0·189	0·192	b ..	0·006	0·181	0·182	0·185
29	b ..	0·040	0·186	0·195	0·199	b ..	0·013	0·185	0·188	0·191
30	b ..	0·025	0·196	0·201	0·204	B ..	0·004	0·189	0·190	0·193
31	c_0 ..	0·024	0·181	0·187	0·190	c_0 ..	0·001	0·181	0·182	0·185

Date	May 1946					September 1946				
	Sky	$\delta'-\delta''$	x	$x_{D\theta}$	x_D	Sky	$\delta'-\delta''$	x	$x_{D\theta}$	x_D
1	b	−0·008	0·187	0·185	0·188	z	−0·006	0·170	0·169	0·172
2	b	−0·011	0·185	0·183	0·186	b	−0·006	0·175	0·174	0·177
3	b	−0·011	0·183	0·181	0·184	b	−0·005	0·179	0·179	0·182
4	z	−0·020	0·184	0·180	0·183	b	−0·005	0·179	0·179	0·182
5	z	−0·006	0·187	0·185	0·189	z_0	−0·002	0·178	0·178	0·181
6	b	+0·008	0·183	0·185	0·188	b	+0·001	0·176	0·177	0·180
7	b	+0·004	0·181	0·182	0·185	b	+0·003	0·179	0·179	0·182
8	b	−0·008	0·188	0·186	0·189	z_0	−0·003	0·176	0·175	0·179
9	c_0	−0·021	0·186	0·182	0·185	b	−0·003	0·180	0·179	0·182
10	z	−0·007	0·187	0·186	0·189	b	−0·007	0·177	0·175	0·178
11	Z	−0·036	0·185	0·177	0·180	b	+0·020	0·176	0·181	0·184
12	z	−0·015	0·182	0·179	0·182	c_0	+0·002	0·169	0·169	0·173
13	z	−0·024	0·184	0·179	0·182	c	..	..	..	..
14	z	−0·023	0·185	0·181	0·183	c	+0·013	0·166	0·169	0·172
15	z	−0·022	0·187	0·183	0·186	o	..	..	..	..
16	z	−0·042	0·188	0·179	0·182	B	−0·007	0·179	0·178	0·181
17	z	−0·018	0·184	0·180	0·183	z	−0·006	0·180	0·179	0·182
18	z	−0·013	0·186	0·183	0·187	b	−0·004	0·178	0·178	0·181
19	Z	−0·060	0·186	0·174	0·176	b	−0·002	0·175	0·175	0·178
20	z	−0·014	0·183	0·180	0·183	B	−0·005	0·179	0·178	0·181
21	z	−0·011	0·186	0·184	0·187	B	−0·005	0·181	0·180	0·183
22	z	−0·010	0·194	0·192	0·196	b	0·000	0·176	0·176	0·178
23	z_0	−0·009	0·194	0·192	0·195	b	−0·003	0·176	0·175	0·178
24	B	−0·005	0·191	0·190	0·193	z_0	−0·006	0·178	0·177	0·180
25	b	+0·008	0·194	0·196	0·199	b	−0·006	0·177	0·176	0·179
26	z_0	−0·011	0·192	0·190	0·193	B	−0·003	0·175	0·175	0·177
27	z	−0·010	0·189	0·187	0·191	B	−0·003	0·173	0·173	0·175
28	o	..	..	..	..	B	−0·003	0·173	0·173	0·175
29	Z	−0·018	0·195	0·191	0·195	B	0·000	0·175	0·175	0·178
30	o	..	..	..	..	B	−0·002	0·179	0·179	0·182
31	b	−0·007	0·198	0·197	0·200					

656·48. Printed at The Bangalore Press, Bangalore City, by G. Srinivasa Rao, Superintendent;
and Published by The Indian Academy of Sciences, Bangalore

NOTICE TO AUTHORS

Scientific papers intended for publication in the *Proceedings of the Indian Academy of Sciences* can be accepted only when they are communicated by Fellow of the Academy whose duty shall be to satisfy himself that such communications are fit to be read at the Meeting of the Academy and published in its *Proceedings*.

Papers should not ordinarily exceed fifty pages of foolscap. MSS. should be either typewritten or written in legible hand on one side of the paper. All papers should be carefully revised by the authors and should be absolutely in final form for printing. Position for text-figures should be indicated. Each paper shall conclude with a critical summary not exceeding 350 words.

Drawings, diagrams or other illustrations should be made on larger scale (preferably) twice the size than the ones in which they are intended to appear. They should be done in Indian ink on bristol board with lettering in pencil. Scale of magnification of camera lucida tracings should be indicated by the side of drawings. In certain special cases arrangements will also be made for monochrome lithographic and other colour plates. Reduction of illustrations desired should be indicated in pencil. Appropriate legends should accompany all drawings. Names of authors are to be marked in pencil on the left-hand corner of drawing sheets. Photomicrographs should be securely mounted with colourless paste.

All tables, quotations and footnotes which will be set hereafter (beginning from Vol. I, No. 2) in types smaller than the text, should be typewritten on separate sheets and placed with the text in proper sequence. Footnotes should be numbered in Arabic numerals.

References to literature in the text should be given, whenever possible, in chronological order, only the names of authors and years of publication, in brackets, being given. They should be cited in full after the summary, the authors' names following in alphabetical order. Thus,

Name or Names of author; Name of Journal (abbreviation) with a single underline; Year of publication; Number of Volume with a double underline, and lastly page. The following would be a useful illustration:—

Bergmann and Stather . . . . . Z. Physiol. Chem., 1926, 152, 189.

Two copies of slip-proof and wherever possible, a page proof for final revision will be sent to authors. All corrections are best made on the slip-proof which should be transmitted to the Office of the Academy. All proof corrections involve heavy expenses which would be negligible if the papers are carefully revised by the authors before submission.

Authors will be supplied with reprints of their papers at cost price, if intimation is given at the time of returning the slip-proof.

All the blocks printed in the *Proceedings* will be offered to the respective authors at a price of 25% of the actual cost of preparing the blocks *plus* the packing and postal charges or railway freight to be incurred for despatching them, it being understood that authors should give due acknowledgment to the Academy whenever such blocks are reproduced in other journals.

The original drawings and plates of blocks appearing in the *Proceedings* will be returned to such of the authors as may require them provided the cost of despatching such originals is borne by them.

CONTENTS

PAGE

Nuclear Oxidation in the Flavones and Related Compounds. Part XIV. Constitution of Quercetagitrin . S. RAJAGOPALAN AND T. R. SESHADRI 31

Influence of Temperature on the Raman Spectra of Crystals. Part III. Barytes . . . . . P. K. NARAYANASWAMY 40

Effect of Dust and Haze on the Spectral Distribution of Zenith-Scattered Radiation . . . . . R. V. KARANDIKAR 46

Diffraction of Light by Very High Frequency Ultrasonic Waves: Effect of Tilting the Wave Front. . . . . S. BHAGAVANTAM AND B. RAMACHANDRA RAO 54

Studies in Atmospheric Ozone. Part II. Daily Measurements of Atmospheric Ozone and of (δ'-δ''), a Measure of Atmospheric Turbidity, at Delhi . . . . . R. V. KARANDIKAR 63